Material Science and Solid State Physics Studies With Positive Muon Spin Precession

Virginia State University
Petersburg, Virginia 23803
U.S.A.

Supported by NASA Grant NSG 1342

Progress Report

June 15, 1979.

Carey E. Stronach
Program Director.

MUON HYPERFINE FIELDS IN Fe(Al) ALLOYS

C.E. Stronach*/

Viginia State University, *Petersburg VA 23803*

W.J. Kossler, J. Lindemuth,† and K.G. Petzinger

The College of William and Mary, Williamsburg VA 23186

A.T. Fiory and R.P. Minnich

Bell Laboratories, Murray Hill NJ 07974

W.F. Lankford

George Mason University, Fairfax VA 22030

J.J. Singh

NASA Langley Research Center, Hampton VA 23665

and

K.G. Lynn

Brookhaven National Laboratory, Upton NY 11973

RECEIVED FEB 8 1979.

*/ Present address: Nuclear Research Centre, University of Alberta, Edmonton, Alberta, Canada T6G 2N5.

† Present address: Siemens Corporation, Cherry Hill NJ 08003

Abstract

The hyperfine field on the muon, B_{hf}, at interstitial sites in dilute Fe(Al) alloys has been measured for four different concentrations of Al and as a function of temperature by the muon spin rotation method. The magnitude of B_{hf}, which is negative, decreases at rates ranging from 0.09 ± 0.03% per at.% Al at 200 K to an asymptotic limit of 0.35 ± 0.03% far above 440 K. This behavior shows that sites near the Al impurity are weakly repulsive to the muon, with an interaction potential of 13 ± 3 meV. In order to fit the temperature dependence of the hyperfine field, it is necessary to hypothesize the existence of a small concentration of unidentified defects, possibly dislocations, which are attractive to the muon. Although the Al impurity acts as a non-magnetic hole in the Fe lattice, the observed decrease in B_{hf} is only 35% of the decrease in the bulk magnetization. We conclude that B_{hf} is determined mainly by the enhanced screening of conduction electrons in Fe and Fe(Al). Since the influence of the Al impurity on the neighboring Fe moments is very small, most of the change in B_{hf} is therefore attributed to the increase in conduction electron polarization at the Al impurity. [PACS 75.50.Bb].

1. Introduction

Knowledge of the local electronic structure around the isotopes of hydrogen, when present as impurities in metals and alloys, is fundamental to a basic understanding of the diffusion of these particles and their poorly-understood interaction with defects and impurities, particularly in Fe. Measurements of the Fermi contact or hyperfine field on positive muons can help provide this information [1-3]. We have studied Fe(Al) alloys with muon spin rotation methods (μSR) to help formulate a physical picture of the local magnetic field and how the host electrons participate in screening the muon's positive charge. Information is also obtained on the mutual interaction between the positive muon and the Al impurities in the Fe host.

The muon probes the magnetic fields at interstitial sites, so that it is specifically sensitive to the extent to which electron states in metals are delocalized, or band-like. As an example of how this is accomplished, we refer to the recent work of Hayano et al. who have compared μSR and host NMR measurements in a study of the itinerant magnetism of the helimagnet MnSi [4]. General applicability of this aspect of such measurements is of course contingent on being able to correctly account for the perturbation which the muon creates in the metal. The problem appears to be tractable and several theoretical approaches have been advanced [1-3,5]. The pure elemental ferromagnets Ni [6-10], Fe [6,7,9-12], Co [7,9,13,14], Gd [15,16], and Dy [17] have been among the metals studied with muons.

The basic properties of the muon in metals may be derived from the assumption that the s-like conduction band electrons are mainly responsible for screening the muon's charge. This interpretation has been proposed for the case of Ni [1,2] assuming d-like states contribute very weakly to the screening at the muon site, even though there is a high density of d states at the Fermi level. However, the s-like bands of Ni have little or no polarization, and the muon therefore experiences a negative hyperfine field which is dominated by the tails of the minority-spin d-like wavefunctions in the

interstitial region. The theoretical basis for this model was discussed by Petzinger and Munjal [1] and by Petzinger [2]. This model takes the opposite view to what had been previously supposed for hydrogen in transition metals [18]. Patterson and Keller [5] recently carried out a finite cluster calculation which lends additional support to this model, in that the d-electrons remain on the neighboring Ni atoms in the cluster.

The above model is thought to be applicable to Fe in spite of the more complicated band structure, where more significant s-d hybridization is found [19]. Jena has discussed the non-linear screening of the muon in Fe in terms of a free-electron gas [3], where the ambient spin density is increased by a factor of 9.8. The measured hyperfine field on the muon is -11 kG, so that on applying this model one finds that the ambient polarization density is effectively $-0.014\,\mu_B$Å^{-3}. By comparison, neutron diffraction measurements [20] give a value of $-0.014 \pm 0.004\,\mu_B$Å^{-3}, averaged over a 0.5 Å cube centered at the tetrahedral interstitial site where the muon is presumed to reside [21]. The neutron data also show that there is a delocalized background polarization of $-0.21\,\mu_B$ per atom, which is equivalent to a homogeneous polarization density of $-0.018\,\mu_B$Å^{-3} [18]. This indicates that the muon hyperfine field is obtained following two quite different assumptions, that the muon experiences either the average conduction electron polarization or the local polarization at a particular site. Band structure calculations have found that the 4s electron contribution to the polarization is between -0.04 and $-0.07\,\mu_B$ per atom [19]. This does not include the contribution from itinerant d states, which is apparently larger. Thus, our view is that previous work indicates that itinerant states in Fe might be treated as a free electron gas in screening the muon.

Alloys of various non-transition elements in Fe have been studied by bulk magnetization measurements [22,23], neutron diffraction [24,25], NMR [26-29] and the Mössbauer effect [29-31]. These measurements found that the Al impurity produces simple magnetic dilution. Neutron diffraction studies have confirmed that the Al is

non-magnetic and that the surrounding Fe neighbors exhibit very little perturbation on their moments. The NMR and Mössbauer satellite lines have been associated with Al in various neighbor shells around the Fe. Grüner et al. [29] have shown that these results can be explained by the spin-polarized conduction electron cloud around the Al. More recently, Terakura has proposed a theoretical explanation based on an ab initio calculation of the electronic densities and polarizations at the Al site [32]. He found a net increase in the s-p polarization at the Al site. His predictions for Si impurities are quite similar to those for Al.

This paper is an elaboration and an extension of our previous studies of Fe(Al) with muons [33]. Additional studies of ferromagnetic alloys were recently reported by Kossler et al. [34] for Ni(Co) and Ni(Cu) and by Nishida et al. [35] for Ni(Cr), Fe(Si) and Fe(Ti).

2. Experiment

μSR is a perturbed angular distribution technique and it has been discussed extensively in the literature [6,36,37]. Spin-polarized positive muons are implanted into the sample under investigation and the time intervals for individual positron decays are recorded. The anisotropy of the positron decay and the precession of the muon spin in the local magnetic field give rise to an oscillatory component in the time dependence of the measured positron emission rate in a given direction. The present studies were done at zero external magnetic field on the samples and used positron detectors at 0° and 180° with respect to the μ^+ beam. The time distribution of the positrons is given by the following formula:

$$N_{e^+}(t) = N_o \exp(-t/\tau_\mu)[1 + a + b\exp(-\lambda t)\cos(\omega t + \phi)] + N_{back} \qquad (1)$$

N_o is an overall normalization, τ_μ the muon lifetime of 2.2 μsec, λ the depolarization

rate, ω the spin precession angular frequency and ϕ a geometrical phase, essentially the angular coordinate of the positron detector. The values of a and b depend upon the distribution of the orientations of the local fields in the sample and upon the angle subtended by the detector [37]. Taking the case of an unmagnetized ferromagnetic sample, where the local fields are isotropically distributed, and longitudinal placement of the detector, we have $a = P/3$ and $b = 2P/3$, where P is a function of the polarization of the muon beam and the energy dependence of the positron detection efficiency [37]. For our experiment $P \approx 0.1$. The term N_{back} is included to account for accidental background counts in the data.

The experiments were performed at temperatures ranging from 80 to 433 K. The data were fitted with Eq.(1) using a multi-parameter least-squares fitting routine. We did not attempt to find the term proportional to a, but rather include it into the definition of N_o and b in fitting the data. The field on the muon is given by $B_\mu = \omega \gamma_\mu^{-1}$, where $\gamma_\mu = 8.51 \times 10^4 \text{sec}^{-1}\text{G}^{-1}$.

Four spherical samples were fabricated, one of 99.99%-pure Fe, the others containing 1.60, 4.29 and 5.81 at.% Al. The sample materials were melted in a MgO crucible in a He atmosphere by rf induction. The Al was added by including Fe(Al) alloy in the melt. The melt was poured into an Al_2O_3-coated Fe mold and allowed to cool in the furnace. The castings were 6 cm in diameter and 20 cm in length. Each casting was reheated to 1273 K and hot pressed, reducing the length by a factor of 2. This is a standard procedure for removing most of the casting structure in Fe and its alloys. The castings were then machined to 5.715 ± 0.001-cm-diameter spheres and annealed in H_2 at 1088 K for one hour. At the concentrations used here, the Al is in a random solid solution [38]. The results of a chemical analysis on the samples is given in Table I. After the μSR runs, the spheres were sectioned for analysis. The sizes of the macroscopic crystallites vary between 0.1 and several mm. The 4.29%-Al sample contains, in addition, dispersed Al_2O_3 precipitates on the order of 1 μm across, which

accounts for the high oxygen concentration in the analysis (There is a thermite reaction between aluminum and oxygen). From transmission electron microscopy, the dislocation density is on the order of $10^8 cm^{-2}$ and the subgrain cells are about 1 μm accross.

3. Data Analysis

3.1 Extraction of the Hyperfine Field

The results for the magnetic fields on the muon and the depolarization rates are listed in Table II. Values of B_μ given in brackets were obtained by linearly interpolating the temperature dependence of the results on pure Fe given by Nishida et al. [11]. The hyperfine fields were extracted in the following manner.

The field experienced by the muon may be decomposed [39] into

$$B_\mu = B_{ext} - B_{DM} + B_L + B_{dip} + B_{hf}, \tag{2}$$

where B_{ext} is the applied external field, B_{DM} is the demagnetizing field which depends upon sample geometry, B_L is the Lorentz cavity field $4\pi M/3$ where M is the domain magnetization, B_{dip} is the sum of the dipole fields inside the Lorentz sphere, and B_{hf} is the Fermi contact or hyperfine field. Because we performed the experiment with zero external field, and since the μ^+ particles hop rapidly from site to site, averaging B_{dip} to zero, the expression for B_{hf} reduces to

$$B_{hf} = B_\mu - B_L. \tag{3}$$

The temperature dependence of the Lorentz cavity field was computed following the parameterization of magnetization data for pure Fe given by Redi [40]:

$$M = M_o f(T) = M_o [1 - A(T/T_c)^{3/2} - B(T/T_c)^{7/2}], \tag{4}$$

where $A = 0.102 \pm 0.005$, $B = 0.33 \pm 0.07$, and $M_o = 1749$ G. We have assumed that the temperature dependence scales with the Curie temperature of the alloy, given as [41]

$$T_c = T_{co}(1 - 0.1\,c), \tag{5}$$

where $T_{co} = 1044$ K is the Curie temperature of pure Fe and c is the Al concentration. The magnetization is also corrected for the presence of Al in the sample by summing the effects of simple dilution, i.e., replacing Fe atoms with Al atoms and taking into account the known change in lattice spacing [42]. The change in lattice spacing Δa_o gives a density factor $3\Delta a_o/a_o$ which becomes $0.157\,c$. Combining these factors yields

$$B_L = \frac{4\pi M}{3}(1 - 1.157\,c), \tag{6}$$

with M given by Eq.(4).

The resulting values of B_{hf} are listed in Table II. The data for sphere No.1 are consistent with pure Fe data of Nishida et al. [11]. The data and fit for B_{hf} at 301 K as a function of concentration are plotted in Fig. 1. The change in B_{hf} is -0.234 ± 0.004 per at.% impurity at 301K.

The reduced quantity $\Delta B_{hf}/c\,B_{hf}$ for $c = 0.0429$ is plotted as a function of temperature in Fig.2. Muon precession oscillations were observed only at 200 K and above, presumably because the muons are trapped at defects below about 200 K. It is seen that the fractional change in hyperfine field is temperature dependent.

3.2 Temperature Dependence of B_{hf}

The temperature dependence of the change in B_{hf} with Al concentration (Fig.2) can be explained if the diffusing muons do not randomly sample the interstitial sites in the alloy. This does not invalidate the assumption that B_{dip} averages to zero because the preference in sampling relates to the presence of an Al nearest neighbor rather than to the two magnetically inequivalent tetrahedral interstitial sites. In general, the average hyperfine field is obtained by summing local contributions from all available sites, weighted according to

Boltzmann population factors:

$$B_{hf} = \sum_i B_{hf}^i \exp(-\beta E^i) / Z, \tag{7}$$

where $\beta = (kT)^{-1}$, E^i the state energies of the muon at sites i, B_{hf} the local hyperfine fields at sites i, and Z the thermodynamic partition function.

In order to give this effect a quantitative treatment, we consider the following model. Firstly, we assume that the E^i vary significantly only at sites immediately adjacent to impurities and defects. Secondly, we assume that the muon energy is changed by an amount E' for a fraction c' of sites which are near the Al impurity. Defects are taken into account by including a fraction c'' of sites with energy E'' relative to the unperturbed sites. Since there are 24 tetrahedral interstitial sites around each Al atom, as opposed to the 6 tetrahedral sites per Fe atom, we take $c' = 4c$, for consistency. If we write the field near the Al sites as B_{hf}', the field at the defect sites B_{hf}'', and the field elsewhere as B_{hf}^o, then the average hyperfine field is given by

$$\Delta B_{hf}/B_{hf}^o = [f' c' \exp(-\beta E') + f'' c'' \exp(-\beta E'')]$$

$$/[1 - c' - c'' + c' \exp(-\beta E') + c'' \exp(-\beta E'')], \tag{8}$$

where we have used the reduced parameters

$$f' = 1 - B_{hf}'/B_{hf}^o$$

and

$$f'' = 1 - B_{hf}''/B_{hf}^o.$$

The data of Fig.2 were fitted with Eq.(8) by treating f', f'', c'', E', and E'' as adjustable parameters. The results are listed in Table III.

We find that the rapid dependence of $\Delta B_{hf}/c\,B_{hf}$ near 250 K, followed by a comparatively gentle dependence at higher temperatures, can therefore easily be explained in terms of a small concentration of strongly attractive defect sites and weakly

repulsive Al sites. The reduced χ^2, for 3 degrees of freedom, is 0.54 for the fit given in Table III. For comparison, we also tested an alternative fit to the data by omitting the defect term, *i.e.*, with $c'' = 0$. The asymptotic value of $\Delta B_{hf}/c\,B_{hf}$ turns out to be 40 % larger and E'' a factor of 2 larger. However, the reduced χ^2, for 6 degrees of freedom, increases to 10. The statistical probability that the defect term gives a better fit is therefore 0.99.

The asymptotic value of B_{hf}/cB_{hf} approaches -0.35 ± 0.03 at very high temperatures (it is -0.31 at the Curie point, 1043K), and we take this to be the average hyperfine field shift for random sampling by the muon. The hyperfine field on the muon at sites near Al is weaker by $8 \pm 1\%$ with respect to pure Fe. The three parameters characterizing the defect sites might be determined better if we had more data in the low-temperature region. We therefore regard these values as approximate. From the small value of the defect concentration found in the fit, $c'' \approx 10^{-9}$, it seems that dislocations and subgrain boundaries would be the likely explanation. Our result does, however, indicate that the shift in the hyperfine field with impurity doping can be developed as a technique for studying the muon-impurity interaction. It could be complementary to depolarization measurements which study the motional narrowing effect of muon motion [9-12]. These points are discussed further in the following sections.

3.3 Depolarization Rates

The μSR signal is observable in Fe and Fe(Al) when the rapid motion of the muon nearly averages out the dipolar field. From the depolarization rate the correlation time of the local dipolar field on the muon can be calculated, and this is nearly the same as the mean time of stay at an interstitial site. The second moment of the dipolar field distribution is about $\overline{(\Delta B_{dip})^2} = (2.6\,\mathrm{kG})^2$, owing to the existence of two magnetically inequivalent tetrahedral sites in pure Fe [10]. The value is nearly the same for the Fe(Al) alloy, although the spatial distribution differs. The depolarization

rate measured at 301 K for our samples is about a factor of 10 larger than those measured in high-purity Fe [12] and does not appear to be very sensitive to the Al concentration. Since samples of Fe of nominally lesser purity typically show larger depolarization rates, this effect has been attributed to longer mean times of stay for muons at sites near or at defects. We could assume, therefore, that the diffusing muons spend part of their lifetime sampling some kind of defect sites throughout the temperature range covered. Clues as to the nature of these defects are obtained by comparing the hyperfine field shift and depolarization data. The fact that the depolarization in the alloys is weaker than for our pure Fe may be due to the scavenging of impurities such as oxygen and nitrogen by the aluminum.

The depolarization measurements for the 4.29 % alloy given in Table II show a monotonic decrease with temperature, with a tendency towards saturation at high temperatures. Thus it appears that the mean time of stay decreases steadily with temperature and that there is a background contribution to the depolarization rate. We consider expressing these data as follows:

$$\lambda = \gamma_\mu \overline{(\Delta B_{dip})^2} f^2(T) \tau_c + \Delta B f(T). \qquad (9)$$

The first term represents the motionally-narrowed local dipolar inhomogeneity and the second term the macroscopic magnetization inhomogeneities. τ_c is a correlation time, which we assume has an Arrhenius temperature dependence:

$$\tau_c = \tau_o \exp(U/kT). \qquad (10)$$

The function $f(T)$ is the same as that given in Eq.(4) and it is included in Eq.(9) in order to correct for the temperature dependence of the dipolar fields. The data do not show any evidence for diffusion limited capture by deep traps (no de-trapping), which would have a τ_c^{-1} dependence [43,12]. A trapping term had been considered by Kossler et al.[43] in their interpretation of the non-Arrhenius temperature dependence of the depolarization rate in Cr and by Nishida et al.[12] in a study of Fe.

The results of a non-linear least-squares fit of Eqs.(9) and (10) to the depolarization data yields the Arrhenius plot of the correlation time given in Fig.3. The parameters of the fit are $\Delta B = 8.8 \pm 0.2\,\mathrm{G}$, $\tau_o = 0.3\,\mathrm{ps}$, and $U = 0.11 \pm 0.02\,\mathrm{eV}$. The statistical uncertainty in τ_o is about a factor of 10.

We note that the activation energy U for the muon jump processes is about a factor of 4 smaller than the magnitude of the defect interaction energy E'' (see Table III) found in the fit of the hyperfine field shift. This difference needs explanation. One consistency check concerns whether the muon jump rate is high enough for the muons to reach the defects. A fair test can be made at $T = 250\,\mathrm{K}$, where the change in the hyperfine field with temperature is most rapid. At this temperature $c'' \exp(-\beta E'') \approx 1$, with muons spending about one-half their time at the defect sites, according to our previous analysis. It can be readily estimated that over the mean duration of the measurement, which is $\lambda^{-1} \approx 0.3\,\mu\mathrm{sec}$ at 250 K, the muon executes $N \approx \lambda^{-1}\tau^{-1}$ jumps, where τ is the jump time. A possible value for τ is 5 ps, obtained by Nishida et al. [12] for high-purity Fe at 250 K, with the result $N \approx 6\times10^{4}$. Equilibrium sampling of defects would be approached when $N c'' \approx 1$. On the contrary, we find $N c'' < 10^{-4}$. To resolve the apparent discrepancy we propose the following: (a) The defects are dislocations and subgrain boundaries, whose effective site concentration is very small; (b) E'' is some average muon-dislocation binding energy; (c) the muons are mobile along the dislocations, with an activation energy of migration U; and (d) the muon mean time of stay at unperturbed interstitial sites in Fe is probably much smaller than 5 ps at 250 K.

4. Discussion

A simple view of the effect of dilute Al impurities is first that the Al is substitutional in Fe and the contribution from the d-states of the removed atom can be simply subtracted. Invoking the observation that the moments of the Fe atoms are nearly unperturbed, we then assume that the d-electron contribution to the average hyperfine field on the muon is simply decreased by 1 % per atomic per cent Al. Further support for this assumption comes from the fact that the magnetic disturbance has only a weak dependence on the valence of the impurity atom [24,25]. There is a similarly small perturbation on the neighboring Fe moments for Si impurities, which have a valence difference of 3 with respect to Fe [25]. The valence difference is 2 for Al. Terakura [32] has discussed the d-band filling and emptying effects for non-transition element impurities in Fe and concludes that these nearly cancel each other. Simple dilution of the d-electron contribution to the hyperfine field on the muon, if that were the main contribution, would lead to $\Delta B_{hf}/c\, B_{hf}$ of -1.0 which is three times larger than the data indicate. The apparent disagreement can be resolved with an explanation in terms of the contribution from conduction electrons.

NMR and Mössbauer measurements have found that the hyperfine field on Fe nuclei at sites nearest neighbor to Al impurities is less negative by 7 % and this has been attributed to a small reduction in the local, negative conduction electron polarization [29]. At the Al site, the conduction electron polarization is negative due to the negative hyperfine field on the Al [40]. From a different point of view, Stearns has treated the pick-up of conduction electron polarization at impurities from the neighboring Fe atoms in terms of the volume misfit of the impurity atom [44,45]. This effect is small for the Al impurity and can be neglected. Referring to the theoretical results calculated by Terakura [32], the fractional change in the s-electron polarization within the Wigner-Seitz sphere at the Al is $+0.08$ and the p-polarization change is -0.03, for a total of $+0.05$. These findings can be used to make a prediction for the

change in the average B_{hf} for muons per unit concentration of Al impurity, taking into account the free electron spin density enhancement factor of 9.8:

$$\Delta B_{hf}/c = 9.8 \frac{8\pi}{3} [0.05 \times 2\mu_B/a_o^3] = 3.3\,\text{kG}. \tag{11}$$

This is equivalent to $\Delta B_{hf}/c\, B_{hf} = -0.30$ and is close to the measured asymptotic value of -0.35 ± 0.03.

The average change in the hyperfine field at the Fe sites in Fe(Al) has been given by several authors [46,47]. The fractional change is in the range -0.4 to -0.5.

Nishida et al. [35] have recently measured B_{hf} for Fe doped with 5% Si at 300K. They find $B_{hf}/c\, B_{hf} = -0.24$. This is the same as the value we find for our 301 K measurements on Fe(Al). Although the asymptotic limit was not checked in the Fe(Si) measurement, this result suggests an insensitivity to the valence difference between Al and Si [30]. The magnetic properties of Fe(Al) and Fe(Si) are also similar [27].

Our explanation for the change in the hyperfine field on muons assumes that distortions in the localized d-wavefunction amplitudes at interstitial sites near the Al impurity can be neglected. This is based on the assumption that local changes in electron spin density associated with these states are not enhanced when the muon is present, as is the case for itinerant states. Thus we are assuming that the μ^+ impurity acts in a manner similar to Al and Si impurities by creating minimal magnetic disturbance in their vicinity. Nevertheless, we cannot completely rule out the possibility that the weak dependence of B_{hf} on Al concentration may arise in part from a large increase in the minority-spin d-like wavefunctions at interstitial sites near the Al. It would be interesting, therefore, to investigate the systematic behavior of B_{hf} for other non-magnetic impurities in Fe as well.

Owing to the apparently extreme sensitivity of B_{hf} to attractive defect potentials, it would be interesting to investigate the systematic effects of dislocations and

impurities such as C, O, and N in Fe alloy samples. Our interpretation predicts a logarithmic dependence of the temperature of inflection in Fig. 2 on the defect concentration. This could be tested with deformed alloys.

Our basic conclusion is that one obtains consistency by treating both the local magnetic perturbation around Al impurities [29] and the hyperfine field on the muon [3] as problems of conduction electron screening and spin density perturbation. It is hoped that these measurements will motivate more fundamental calculations for determining the origins of the muon hyperfine field and the local muon potential, such as finite cluster calculations treating the ternary system μ^+-Al in Fe.

Acknowledgments

This work was supported in part by Bell Laboratories, the Commonwealth of Virginia, the Department of Energy, the National Aeronautics and Space Administration, and the National Science Foundation. The alloys were prepared by R.E. Manners at Bell Laboratories and S. Mahajan, G. Dolan, and M. Davis participated in the specimen analysis. The experiments were carried out at the NASA Space Radiation Effects Laboratory, Newport News, Virginia, which was also supported by the National Science Foundation and the Commonwealth of Virginia. The enthusiastic support of R.T. Siegel and the SREL staff is greatly appreciated. P.A. Barnette, D.M. Parkin and W.B. Gauster participated in preliminary μSR experiments on Fe(Al) [33].

References

1. K.G. Petzinger and R. Munjal, Phys. Rev. B 15 (1977) 1560.
2. K.G. Petzinger, Hyperfine Interactions 4 (1978) 307.
3. P. Jena, K.S. Singwi, and R.M. Nieminen, Phys. Rev. B 17 (1978) 301.
4. R.S. Hayano, Y.J. Uemura, J. Imazato, N. Nishida, T. Yamazaki, H. Yasuoka, and Y. Ishikawa, Hyperfine Interactions, to be published.
5. B.D. Patterson and J. Keller, Hyperfine Interactions, to be published.
6. M.L.G. Foy, N. Heiman, W.J. Kossler, and C.E. Stronach, Phys. Rev. Lett. 30 (1973) 1064.
7. I.I. Gurevich, A.I. Klimov, V.N. Maiorov, E.A. Meleshko, B.A. Nikolskii, V.I. Selivanov and V.A. Suetin, Zh. Eksp. Teor. Fiz. 69 (1975) 439 [Sov. Phys. - JETP 42 (1976) 222].
8. K. Nagamine, S. Nagamiya, O. Hashimoto, N. Nishida, T. Yamazaki and B.D. Patterson, Hyperfine Interactions 1 (1976) 517.
9. H. Graf, W. Kündig, B.D. Patterson, W. Reichart, M. Camani, F.N. Gygax, W. Rüegg, A. Schenck and H. Schilling, Helv. Phys. Acta 49 (1976) 730.
10. H. Graf, E. Holzschuh, E. Recknagel, A. Weiginger, and Th. Wichert, Hyperfine Interactions, to be published.
11. N. Nishida, R.S. Hayano, K. Nagamine, T. Yamazaki, J.H. Brewer, D.M. Garner, D.G. Fleming, T. Takeuchi, Y. Ishikawa, Solid State Commun. 22 (1977) 236.
12. N. Nishida, K. Nagamine, R.S. Hayano, T. Yamazaki, R.I. Grynszpan, A.T. Stewart, J.H. Brewer, D.G. Fleming, and S. Talbot-Besnard, Hyperfine Interactions, to be published.

13. H. Graf, W. Kündig, B.D. Patterson, W. Reichart, P. Roggwiller, M. Camani, F.N. Gygax, W. Rüegg, A. Schenck, H. Schilling, and P.F. Meier, Phys. Rev. Lett. 37 (1976) 1644.

14. N. Nishida, K. Nagamine, R.S. Hayano, T. Yamazaki, D.G. Fleming, R.A. Duncan, J.H. Brewer, A. Akhtar and H. Yasuoka, Hyperfine Interactions 4 (1978) 318.

15. I.I. Gurevich, A.I. Klimov, V.N. Maiorov, E.A. Meleshko, B.A. Nikolskii, A.V. Purogov, V.S. Roganov, V.I. Selivanov, and V.A. Suetin, Zh. Eksp. Teor. Fiz. 69 (1975) 1453 [Sov. Phys. - JETP 42 (1976) 741].

16. H. Graf, W. Hofmann, W. Kündig, P.F. Meier, B.D. Patterson, and W. Reichart, Solid State Commun. 23 (1977) 653.

17. W. Hofmann, W. Kündig, P.F. Meier, B.D. Patterson, K. Rüegg, O. Echt, H. Graf, E. Recknagel, A. Weidinger, and T. Wichert, Phys. Lett. 65A (1978) 343.

18. J. Friedel, Ber. Bunsenges. Phys. Chem. 76 (1972) 828.

19. J. Callaway and C.S. Wang, Phys. Rev. 16 (1977) 2095, and references therein.

20. C.G. Shull and H.A. Mook, Phys. Rev. Lett. 16 (1966) 184; C.G. Shull, *Metallurgical Society Conferences, Vol 43: Magnetic and Inelastic Scattering of Neutrons by Metals*, ed. T.J. Roland and P.A. Beck, Gordon and Breach Science Publishers, New York (1967) 15. The ambient value $4\pi M = -1.6$ kG is given for the tetrahedral interstitial site in Fe.

21. A. Seeger, Phys. Lett. 58A (1976) 137.

22. I. Vincze and M.J. Besnus, J. Phys. F: Metal Phys. 5 (1975) 2129.

23. M.J. Besnus, A. Herr, and A.J.P. Meyer, J. Phys. F: Metal Phys. 5 (1975) 2138.

24. M.F. Collins and G.G. Low, Proc. Phys. Soc. 86 (1965) 535.

25. T.M. Holden, J.B. Comly, and G.G. Low, Proc. Phys. Soc. 92 (1967) 726.

26. J.I. Budnick, Colloque Ampère, North-Holland, Amsterdam (1969) 187.

27. M. Rubenstein, G.H. Stauss, and M.B. Stearns, J. App. Phys. 37 (1966) 1334.

28. E.F. Mendis and L.W. Anderson, Phys. Stat. Sol. 41 (1970) 375.

29. G. Grüner, I. Vincze, L. Cser, Solid State Commun. 10 (1972) 347.

30. C.E. Johnson, M.S. Ridout, and T.E. Cranshaw, Proc. Phys. Soc. 81 (1963) 1079.

31. G.K. Wertheim, V. Jaccarino, J.H. Wernick and D.N.E. Buchanan, Phys. Rev. Lett. 12 (1964) 24.

32. K. Terakura, J. Phys. F: Metal Phys. 6 (1976) 1385.

33. C.E. Stronach, P.A. Barnette, W.J. Kossler, K.G. Petzinger, J.J. Singh, A.T. Fiory, W.F. Lankford, W.B. Gauster, and D.M. Parkin, Bull. Am. Phys. Soc. 22 (1977) 78. C.E. Stronach, A.T. Fiory, R.P. Minnich, W.J. Kossler, J. Lindemuth, K.G. Petzinger, W.F. Lankford, J.J. Singh, and K.G. Lynn, Bull. Am. Phys. Soc. 23 (1978) 227.

34. W.J. Kossler, A.T. Fiory, W.F. Lankford, K.G. Lynn, R.P. Minnich and C.E. Stronach, Hyperfine Interactions, to be published.

35. N. Nishida, K. Nagamine, R.S. Hayano, Y.J. Uemura, J. Imazato, T. Yamazaki, H. Miyajima, S. Chikazumi, D.G. Fleming and J.H. Brewer, Hyperfine Interactions, to be published.

36. J.H. Brewer, K.M. Crowe, F.N. Gygax and A. Schenck, *Muon Physics, Vol 3: Chemistry and Solids*, eds. V.W. Hughes and C.S. Wu, Academic Press, New York (1975).

37. A. Schenck, *Nuclear and Particle Physics at Intermediate Energies*, ed. J. Warren, Plenum, New York (1976) page 159.

38. L.D. Khoi, P. Veillet and I.A. Campbell, J. Phys. F: Metal Phys. 5 (1975) 1203.

39. A. Schenck, Hyperfine Interactions 4 (1978) 282.

40. P. Redi, Phys. Rev. B 8 (1973) 5243.

41. G.P. Huffman, AIP Conf. Proc. 5 (1971) 1314.

42. A. Taylor and R.M. Jones, J. Appl. Phys. 29 (1958) 522.

43. W.J. Kossler, A.T. Fiory, D.E. Murnick, C.E. Stronach, W.F. Lankford, Hyperfine Interactions 3 (1977) 287.

44. M.B. Stearns, Phys. Rev. B 13 (1976) 4180.

45. I.A. Campbell and I. Vincze, Phys. Rev. B 13 (1976) 4178.

46. M.B. Stearns, Phys. Rev. B 6 (1972) 3326.

47. J.J. Singh, Bull. Am. Phys. Soc. 21 (1976) 21; NASA TM-72810 (1975); NASA TMX-74067 (1977).

TABLE I. Properties of the Fe(Al) spheres used in this study. The impurity concentrations measured by atomic absorption analysis for Al, by vacuum fusion analysis for C, O, and N, and by mass spectrographic analysis for the other elements, are given in atomic per cent under the element headings. He and H were below the limits of detectability, 0.0001% and 0.0005%, respectively. An additional estimated 0.2 at.% Al is present in sphere No.3 in the form of Al_2O_3 precipitates.

Mass (g)	Al	C	O	N	Si	Ni	Zr	Ti	Mg	Cu
766.91	0.001	0.002	0.64	0.003	0.004	0.005	0.003	0.0005	0.0005	0.0002
760.84	1.60	0.002	0.01	0.003	0.008	0.005	0.003	0.0005	0.0005	0.0002
743.22	4.29	0.013	0.3	0.01	0.008	0.005	0.003	0.0005	0.0005	0.0002
739.88	5.81	0.002	0.01	0.003	0.008	0.005	0.003	0.0005	0.0005	0.0002

TABLE II. Observed magnetic fields on the muon B_μ, muon-spin depolarization rates λ, calculated Lorentz cavity fields B_L, and resultant Fermi-contact hyperfine fields B_{hf}. Errors of measurement are enclosed in parenthesis. Values of B_μ enclosed in brackets were interpolated from the data of Nishida et al. [11]. c is the Al impurity concentration in atomic per cent.

c	T (K)	B_μ(G)	λ (μ sec^{-1})	B_L(G)	B_{hf}(G)
0	200	[−3672(2)]		7256	−10,928
	240	[−3638(2)]		7230	−10,868
	260	[−3621(2)]		7215	−10,836
	280	[−3604(2)]		7198	−10,802
	301	[−3590(1)]		7179	−10,769
	301	−3592(3)	3.0(3)	7179	−10,771
	343	[−3530(4)]		7136	−10,666
	373	−3477(2)	2.2(2)	7101	−10,578
	433	−3379(3)	1.5(1)	7016	−10,394
1.60	301	−3687(2)	1.4(2)	7046	−10,733
4.29	200	−3990(14)	9(2)	6896	−10,886
	240	−3954(5)	3.8(4)	6870	−10,824
	260	−3902(2)	2.9(2)	6856	−10,758
	280	−3866(2)	2.0(1)	6840	−10,706
	301	−3842(2)	1.7(3)	6822	−10,664
	343	−3772(1)	1.5(1)	6781	−10,553
	373	−3719(1)	1.0(1)	6746	−10,466
	433	−3612(1)	1.0(1)	6665	−10,277
5.81	301	−3930(2)	1.3(2)	6695	−10,625

TABLE III. Parameters fitting Eq.(8) to the temperature dependence of the hyperfine field in the 4.29% Fe(Al) alloy. f' and f'' are the fractional changes in the hyperfine field, c' and c'' the site concentrations, E' and E'' the site energies, for Al and defect sites, respectively. The parameter $c' = 4c$ was held constant.

f'	$-0.087(7)$
f''	$-0.0032(8)$
c'	0.172
c''	$10^{-11.7\pm3.6}$
E'	0.013(3) eV
E''	$-0.6(2)$ eV

Figure Captions

Figure 1. The Fermi-contact hyperfine field on the positive muon in Fe(Al) as a function of impurity concentration at a temperature of 301 K. The line is a least-squares fit.

Figure 2. Temperature dependence of the fractional change in the hyperfine field with aluminum concentration. Data were taken for $c = 0.0429$. The curve is the fitted function Eq.(8) divided by c, using the parameters of Table III.

Figure 3. Dependence of the local field correlation time upon inverse temperature, obtained from depolarization rates according to Eqs.(9) and (10). The curve is the fitted function.

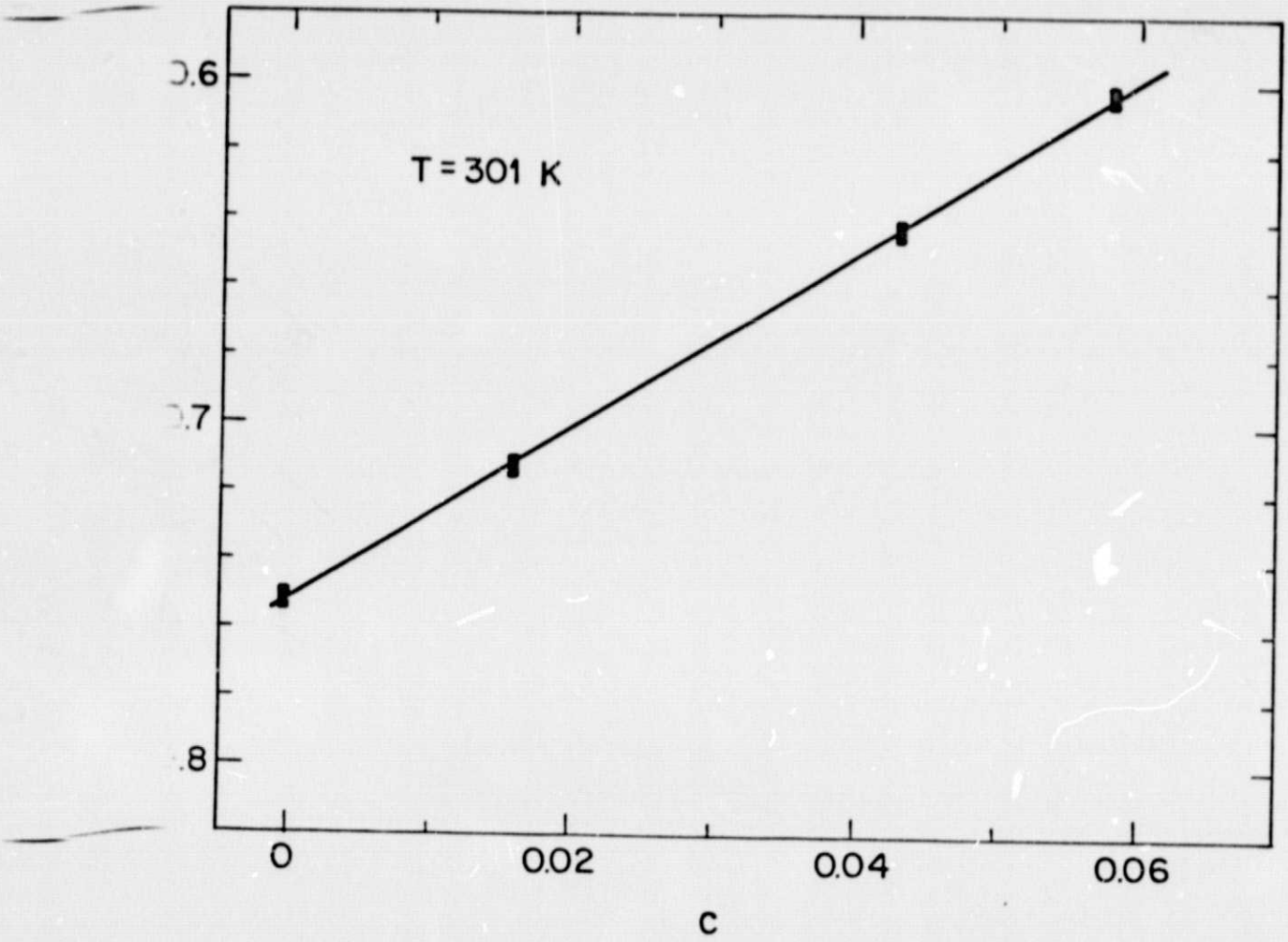

FIGURE 1

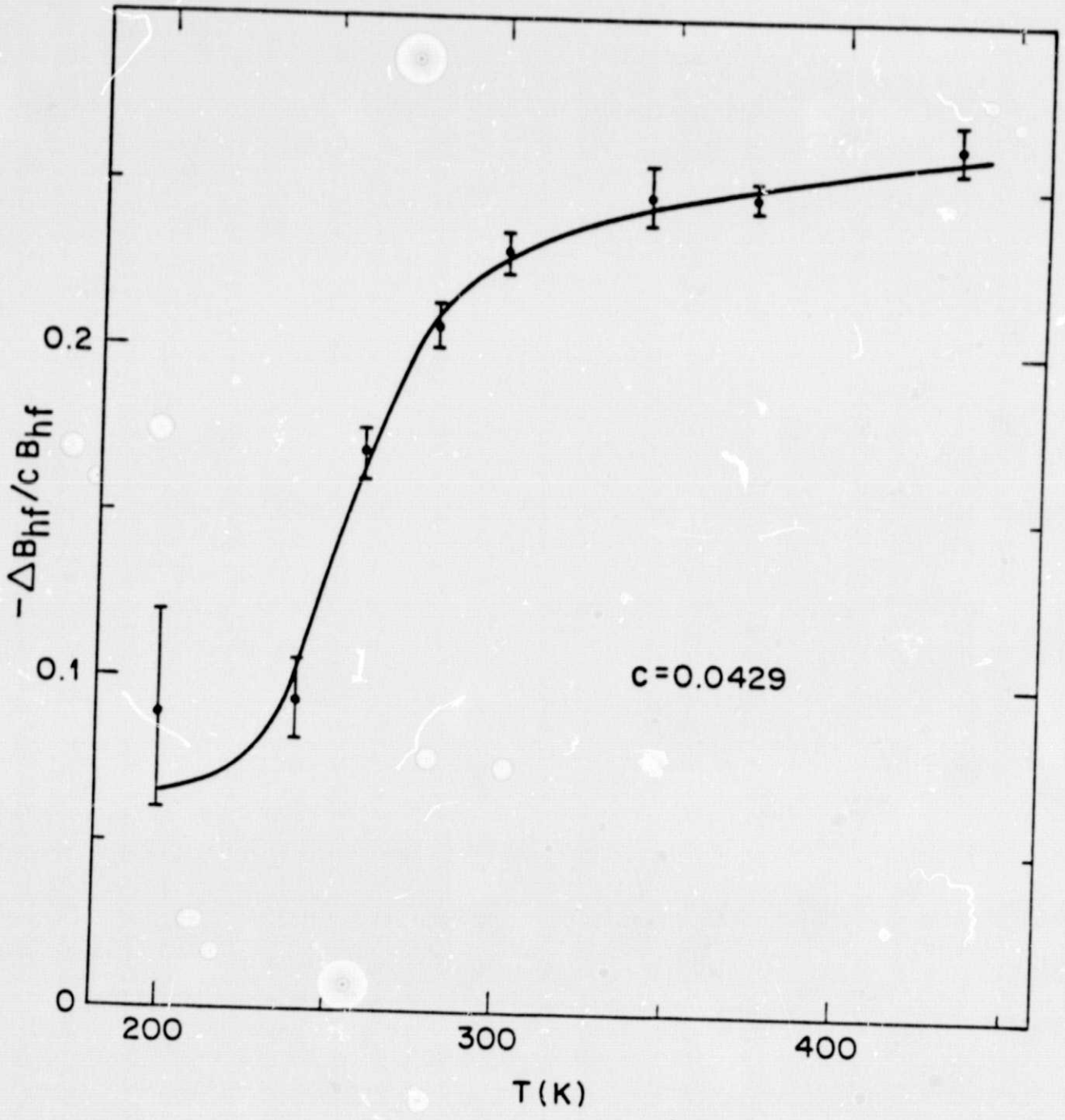

FIGURE 2

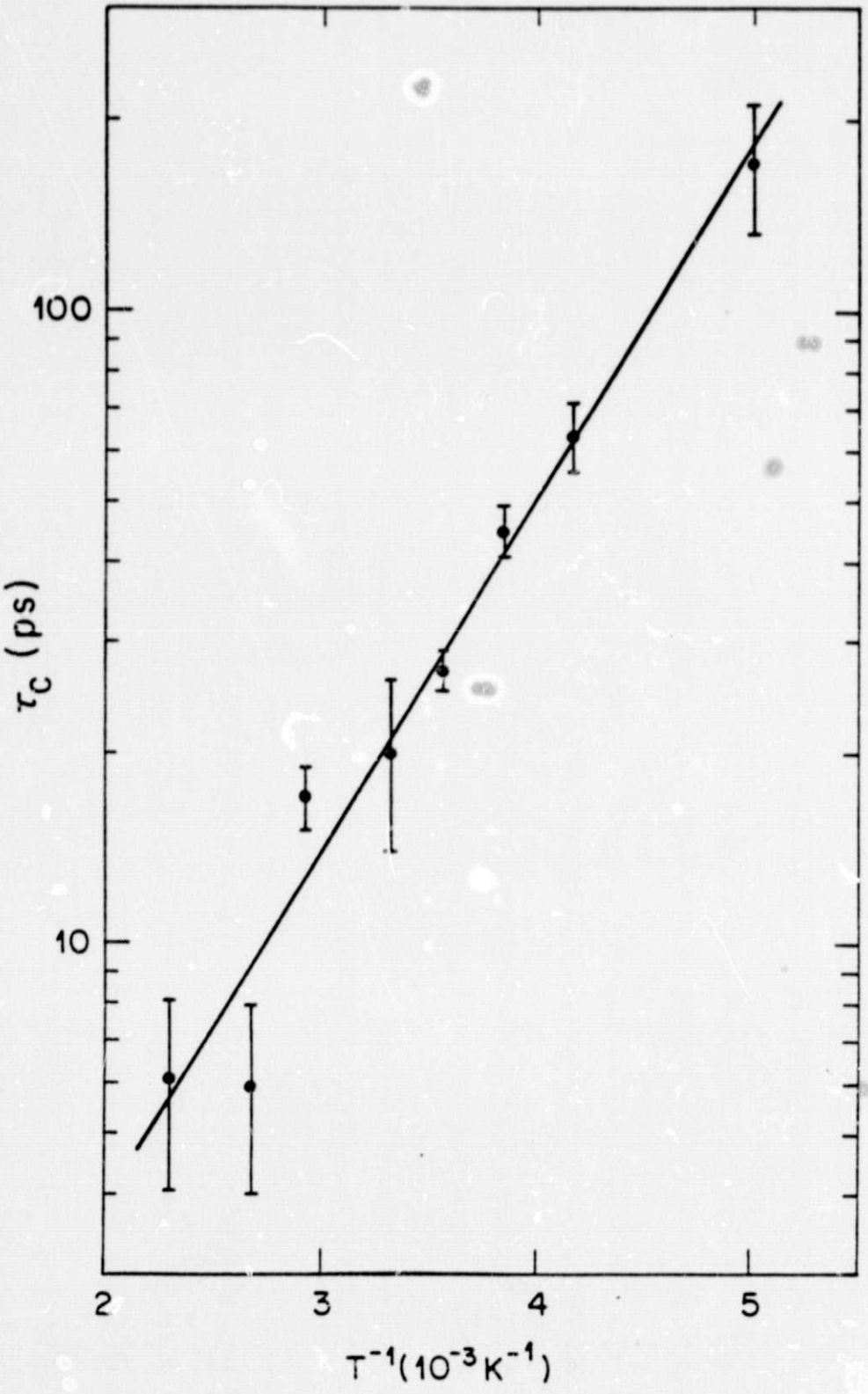

FIGURE 3

Hyperfine Interactions 6 (1979) 93-97

MAGNETIC FIELD ON THE μ^+ IN Ni DOPED WITH 0.76at.% Cu OR WITH 0.76at.% Co FROM 5 to 330K

W. J. Kossler*(a), A. T. Fiory (b), W. F. Lankford*(c),
K. G. Lynn†(d), R. P. Minnich (b) and C. E. Stronach♣(e)

(a) College of William and Mary, Williamsburg VA 23186 USA
(b) Bell Laboratories, Murray Hill, NJ 07974 USA
(c) George Mason University, Fairfax VA 22030 USA
(d) Brookhaven National Laboratory, Upton NY 11973 USA
(e) Virginia State College, Petersburg VA 23803 USA

Measurements of local magnetic fields and depolarization rates were made as a function of temperature in zero external field in samples of Ni alloyed with either 0.76at.% Cu or 0.76at.% Co. At temperatures below 50K the magnetic field on the μ^+ in the Ni-Cu alloy is 1462±2G and for the Ni-Co alloy the field is 1524±7G.

I. Introduction

The purpose of the present study is to determine the effect of either Cu or Co impurities on the magnetic field experienced by the positive muon probe in ferromagnetic Ni. Previous work [1-3] has established that the Fermi-contact or hyperfine field on the positive muon in pure Ni is negative, i.e., it is directed oppositely to the bulk magnetization, and equals -1.1G at low temperatures. The hyperfine field is also only slightly temperature dependent up to room temperature, decreasing by about 1% as the magnetization of Ni decreases by 7% [3]. The muon occupies the octahedral interstitial site, a region that lies in between the Ni second nearest neighbors and where the ambient magnetic field is particularly uniform at about -660G [4].

The magnitude of the contact field has been explained theoretically [5-9] as arising from the negative polarization of the 3d orbitals in the interstitial region. The 4s electrons are mainly responsible for screening the muon's charge and seem to make a negligible contribution to the contact field [10].

In pure Ni the majority d bands are fully occupied and there is a 0.6-electron vacancy in the minority band. The addition of Cu decreases the bulk magnetization by 1.9% per atomic per cent Cu, with a critical concentration of 53%. Locally, the Cu atom is non-magnetic [11], while the moments of the neighboring Ni atoms are decreased. The addition of Co to Ni has the opposite effect: the magnetization increases and the Co retains its magnetic moment.

II. Experimental Procedure

Polycrystalline samples for μSR experiments were prepared from 99.99%-pure starting materials. Two alloys, Ni with 0.76% Cu and Ni with 0.76% Co were cast in a mould, hot pressed to a thickness of 1.6cm, annealed, machined to a final size of 7.6cm × 10.2cm × 1.3cm, annealed again at 550°C for one hour in a hydrogen atmosphere, and cooled overnight in the furnace.

The μSR data were collected at zero external magnetic field for positron decays in the forward and backward directions with respect to the muon polarization. The time histograms were fitted with an exponentially-damped oscillatory function in order to extract the field on the muon, B_μ, and the depolarization rate λ. For comparison, a 99.99%-pure Ni sample was also studied.

---

* Supported in part by the NSF and the Commonwealth of Virginia
† Supported by the Department of Energy
♣ Supported in part by NASA

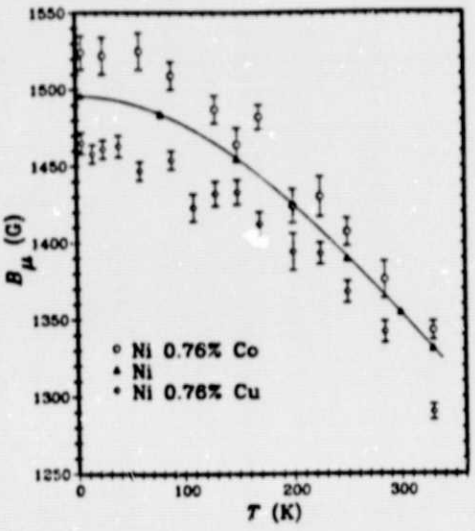

Figure 1. Temperature dependence of the local field on the muon.

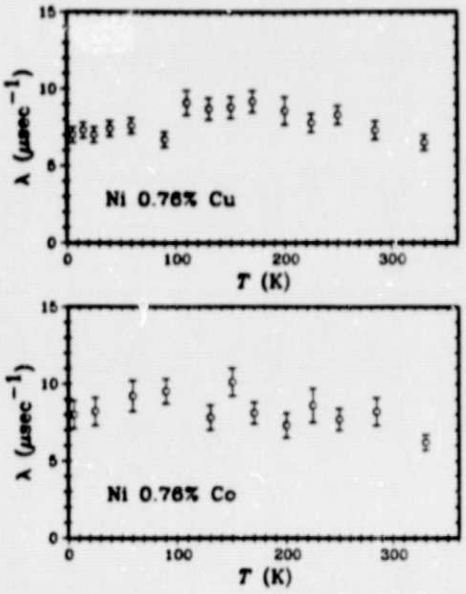

Figure 2. Temperature dependence of the depolarization rate.

III. Experimental Results and Discussion

The temperature dependence of B_μ and λ are given in Figs. 1 and 2. The initial asymmetry in the μSR signal is about 0.12 on the average and does not depend upon temperature, to within the statistical accuracy of 10%. The larger measured depolarization in the alloys, ranging from 6 to 10 μsec^{-1}, permitted less precise determination of B_μ.

The static field broadening associated with the impurities makes a contribution to the depolarization that may depend upon where the muon stops. It tends to be averaged out if the muon is diffusing rapidly. The depolarization rate calculated for the case where the muon stops randomly in the lattice is given by [12]:

$$\lambda = \gamma_\mu 8\pi^2 N c \bar{\mu} / 9\sqrt{3},$$

where N is the density of lattice atoms, $\bar{\mu}$ approximately equals one Bohr magneton, and c is the impurity concentration. For c = 0.0076, we calculate $\lambda = 2.8\ \mu sec^{-1}$. If the muon were to selectively stop at a site adjacent to one of the Cu or Co impurities, the depolarization rate would be about 80 μsec^{-1}. We conclude that the observed depolarization rate is due mainly to macroscopic field inhomogeneities of 70 to 120G. The muons do not appear to be rapidly depolarized by trapping at the Cu or Co impurities. This is ruled out because we do not find any temperatures with an appreciable loss of signal amplitude, as measured by the initial asymmetry.

The sign of B_μ, which has been deduced from previous work [1], is positive and is given by the following formula:

$$B_\mu = 4\pi M_s/3 + B_{hf},$$

where M_s is the saturation magnetization and B_{hf} the hyperfine field. We have assumed that the average magnetic field within a magnetic domain is correctly given by the Lorentz local field, although there may be random contributions

from magnetization inhomogeneities and impurities. Any random fields would contribute to the depolarization rate.

At low temperatures, the values of B_μ for Ni-Cu are smaller than they are for pure Ni, while for Ni-Co they are larger. The differences become less pronounced as the temperature is raised above 100K. The difference in B_μ between Ni-Cu and pure Ni increases again as the temperature is further raised to 330K. There are fluctuations in the temperature dependence of both λ and B_μ which may possibly be significant. The changes evident at 100K occur in the temperature region where the onset of thermal diffusion of the μ^+ is observed in pure Cu [13].

At low temperatures, the $4\pi M_s/3$ field is 30.6G smaller in Ni-Cu than it is in pure Ni. Thus most of the observed decrease of 34.3±4.0G that we find for temperatures less than 50K can be attributed to the decreased macroscopic magnetization, assuming that the muons stop at randomly selected interstitial sites in the alloy. The remainder is due to a change in B_{hf}. Values of the reduced fractional change, $\Delta B_{hf}/cB_{hf}$, are given for the low-temperature and 330K data in the Table.

TABLE. Experimental values for the fractional change in hyperfine field per unit concentration, $\Delta B_{hf}/cB_{hf}$.

	5-60K	330K
Ni-Cu	0.8 (0.8)	2.8 (1.1)
Ni-Co	0.7 (1.5)	3.7 (1.3)

The results at 330K are interpreted with the assumption that the muons diffuse rapidly through the lattice. It is at first sight unusual that the hyperfine field shift at 330K has the same sign for both alloys. To explain this, one could assume the Cu impurity to be repulsive to the muon, so that sites near the Cu would be selectively sampled less frequently by the diffusing muon. The sites near the Co impurity, on the other hand, need to be sampled more frequently. With this interpretation, the results given in the second column of the Table show that the hyperfine field at sites distant from a Cu impurity is larger than it is in pure Ni, while for the Co impurity, sites near the Co have the larger field. A repulsive local potential has recently been observed by Stronach et al. [14], who studied the Al impurity in Fe.

IV. Conclusions

Both our results and the results for pure Ni [1-3] can be interpreted with the model that attributes the hyperfine field on the positive muon in Ni to the local d-band polarization. The field is negative because it is dominated by minority spin bands, whose wavefunctions are more spread out and thus overlap the muon at the octahedral interstitial site. Petzinger has presented arguments showing how the temperature-dependent shift of the hyperfine field in pure Ni is weak because minority-band filling compensates the decrease in the magnetization with temperature [9]. One could suppose that similar arguments apply in the case of alloying with small amounts of Cu.

The data also show that the shift in the hyperfine field at sites near the impurities tends to be opposite to the shift elsewhere, with the result that the average shift is very small. We have presumed that the hyperfine field is weaker near Cu impurities because the local d-band splitting is smaller near Cu impurities. Conversely, the sites adjacent to the Co have a larger hyperfine field, which one might have anticipated since the hyperfine field in pure Co, -6.2 kG, is larger than it is in pure Ni [15]. Our results are also consistent with previous conclusions that the local spin-density enhancement factor is effectively unity for the 3d-like orbitals.

Acknowledgement

The authors thank K. G. Petzinger for stimulating conversations.

References

1. M.L.G. Foy et al., Phys. Rev. Lett. 30, 1064 (1973).
2. I.I. Gurevich et al., Zh. Eksp. Teor. Fiz. 69, 222 (1975) [JETP 42, 222 (1976)] and references therein.
3. K. Nagamine et al., Hyperfine Interactions 1, 517 (1976).
4. H.A. Mook, Phys. Rev. B 148, 495 (1966).
5. B.D. Patterson and L.M. Falicov, Solid State Commun. 15, 1509 (1974).
6. P.F. Meier, Solid State Commun. 17, 987 (1975).
7. K.G. Petzinger and R. Munjal, Phys. Rev. B 15, 1560 (1977).
8. P. Jena, K.S. Singwi and R.M. Nieminen, Phys Rev. B 17, 301 (1978).
9. K.G. Petzinger, Hyperfine Interactions 4, 307 (1978).
10. There is evidence for an s-electron contribution from Knight-shift measurements. See A. Schenck, Hyperfine Interactions 4, 282 (1978).
11. M.H. Bancroft, Phys. Rev. B 2, 182 (1970).
12. R.E. Walstedt and L.R. Walker, Phys. Rev. B 9, 4857 (1974).
13. I.I. Gurevich et al., Phys. Lett. A40, 143 (1972).
14. C.E. Stronach et al., to be published.
15. H. Graf et al., Phys. Rev. Lett. 37, 1644 (1976).

DISCUSSION

D.G. FLEMING:

Since the T dependence of B_{hf} does not follow M(T) depending on impurity concentration, we should be a little cautious in interpreting $B_{hf}^{\mu^+}(T)$ - M(T) as due to the host metal rather than the presence of(unknown)impurities.

A.T. FIORY:

I agree. The possibility that diffusing muons do not randomly sample the sites in the lattice has not been extensively checked. There is some information on this: in Fe doped with Al, the muon-Al repulsion has been observed by Stronach et al. at SREL. A change in the observed Fermi-contact field occurs when C_{imp} exp (E/kT) becomes comparable to unity, where C_{imp} is the impurity concentration and E the muon-impurity binding enthalpy. For trapped muons, self-trapped or otherwise, thermal equilibrium treatment does not apply. For fcc lattice like Ni, the low-temperature data may contain selective trapping anomalies: we do not know at present if that is the case.

Hyperfine Interactions 6 (1979) 295-299

μ^+ DEPOLARIZATION MEASUREMENTS OF Al ALLOYED WITH 0.1 at.% Ag, Cu, Mg, Si, and Zn

W. J. Kossler,[a] A. T. Fiory,[b] W. F. Lankford,[c]
K. G. Lynn,[d] R. P. Minnich,[b] and C. E. Stronach[e]
a) College of William and Mary, Williamsburg VA 23186 USA
b) Bell Laboratories, Murray Hill NJ 07974 USA
c) George Mason University, Fairfax VA 22030 USA
d) Brookhaven National Laboratory, Upton NY 11973 USA
e) Virginia State College, Petersburg VA 23803 USA

To try to understand the nature of μ^+ trapping by impurities in Al, as has recently been observed for copper impurities, Al alloyed with 0.1 at.% Ag, Cu, Mg, Si and Zn has been studied as a function of temperature and heat treatment.

I. Introduction

In high purity, undamaged aluminum muons are observed to not depolarize over the temperature range 2.8 to 300K [1], implying rapid diffusion. On the other hand a small admixture of Cu produces trapping as inferred from temperature-dependent depolarization [2]. The temperature dependence of the depolarization rate has been observed to change with impurity concentration [3], and neutron induced vacancies created and maintained at low temperature have been observed to trap muons [4]. These vacancies disappear somewhere above 220K [5].

It is reasonable to expect that the problem of the muon in aluminum under various circumstances is amenable to calculation. Theoretical predictions for the heat of solution for hydrogen have already been obtained [6]. The relaxation of the lattice due to the muon has been treated by Shaw using pseudopotentials [7]. The extension of pseudopotential theory to include binding to impurities is approachable. The tractability of aluminum is associated with its having only s and p shells filled and having a very small core. The heavier metals do not share this advantage.

The complete temperature structure in the depolarization rate, which has been observed for Al with dilute Cu, would seem to indicate a variety of trapping sites. These sites could be clusters of impurities or impurity-vacancy complexes.

Aluminum can thus be viewed as a medium in which trapping sites can form and which by itself does not trap, suggesting that different impurities be added to it to find muon-impurity binding energies and by the use of differing heat treatments purposely creating different impurity-impurity and impurity-vacancy complexes for which concentrations and detrapping energies might be obtained.

II. Experiment

Appropriate quantities of 99.99% Al and alloying element were melted in an MgO crucible by rf induction heating. The molten alloy was then cast into 2kG ingots, which subsequently were hot rolled to a thickness of 3mm. The molten alloy was handled in a dry helium atmosphere. Rectangular pieces 7.6 × 10.2 cm were then cut out. These samples were heat treated for 8 hours at 800-825K and quenched to 273K in a brine bath with cooling times measured to be between 0.05 and 0.2 second. The samples were stored at temperatures below 200K to avoid thermal aging.

After precession experiments to 330K, the samples were annealed at 800K for 8 hours, then cooled by standing in air so that a time constant of typically 250

seconds was obtained, and again used for precession measurements. These data were designated: air cooled.

Following these measurements, the samples were again heat treated for 8 hours again at 800K, then cooled in the oven with the power off, typically with a time constant of 4 hours. Precession measurements on these samples were designated: oven cooled.

Analysis by mass spectrograph showed the samples to be: Al (0.1 at.% Ag), Al (0.09 at.% Si), Al (0.042 and 0.13 at.% Cu), Al (0.1 at.% Mg), and Al (0.06 at.% Zn). These measurements are expected to be approximately 5% accurate. Residual Cu impurities of 15-30 ppm were seen, as well as possible traces of Si.

Seven or eight 3mm-thick sample plates were stacked inside a cryostat. Temperatures were measured with carbon and platinum resistors and controlled to typically better than 0.1K.

An iron core magnet with shims and trim coils provided a field of 500 G. The measured inhomogeneity was about 25mG over the sample volume and during the μSR measurement the field was controlled by a feedback system to better than 10mG. A continuous record was maintained of any deviation.

Positrons were detected with plastic scintillators at 0° and 180° with respect to the incident beam direction. Both were 20 × 20 cm, the 180° detector having a 6.4-cm diameter hole for the beam to enter. Typical stopping muon rates were 7000 sec^{-1} with event rates of approximately 2000 sec^{-1}. Data were taken for about 45 minutes per point, corresponding to 4 million events. These data were fitted on-line using the usual expression with Gaussian damping of the polarization, $\exp(-\sigma^2\tau^2)$. We have found that the dimensionless parameter:

$$\alpha = \int_0^\infty e^{-st}(d\gamma/dt)dt$$

with $s = 1/\tau_\mu$ and the time dependence of the polarization represented by $\exp[-\gamma(t)]$ is less fitting-model dependent than the 1/e time and more directly calculable in terms of muon correlation functions. For example,

$$\gamma(t) = \sum_i \sigma_i^2 \int_0^t dt' \int_0^t dt F_i(t'')G_i(t'-t'')$$

is a natural representation of the depolarization in terms of the occupation probability $F_i(t)$ and autocorrelation function $G_i(t)$ for site i. As a matter of practice the Gaussian fit to the data is used and then $\alpha = 2\sigma^2\tau_\mu^2$.

III. Results and Discussion

For comparison to the data it is useful to know that α is 0.44 for the muon localized at an octahedral site and 0.12 for a substitutional site neglecting lattice relaxation and distortion of the muon wave-function.

In Al, deformed at 77K, we had previously found [3] depolarization rates consistent with trapping in open volume defects and not at interstitial sites due to the strain fields around the defects. These data are presented in Fig. 1a for reference.

On the other hand, with Cu impurities in Al we had found a concentration dependence to the structure, see Fig. 1b, which indicates stronger trapping for increased impurity density.

The general features seen for Al(Cu) are seen in Al(Si) with peaks occuring in different places. A maximum in α occurs at 2K of 0.2 then α falls linearly to 0.15 at 5K, a peak of 0.2 arises at 10K followed by a plateau of 0.12 between 16

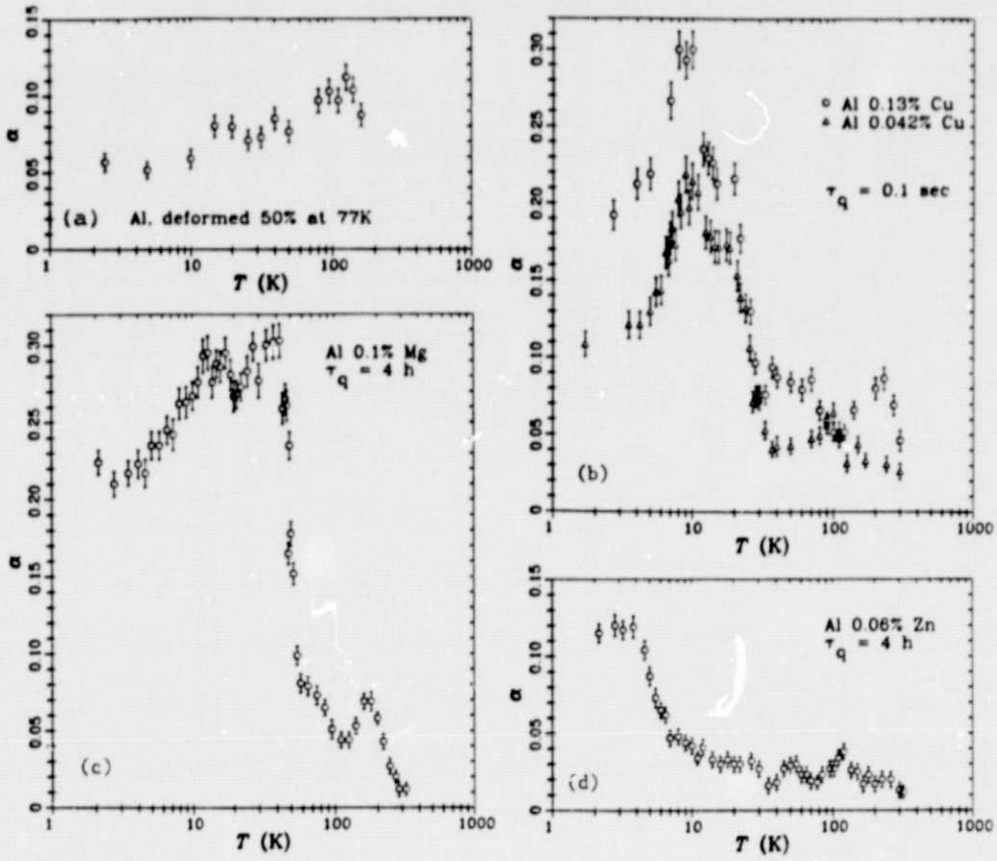

Fig. 1 Temperature Dependence of the Depolarization Rate Parameter.

and 30K, a peak of 0.13 occurs at 35K, followed by a decrease to 0.04 at 120K. A final peak is seen at 180K of 0.07 and by 250K α has been reduced to 0.015.

Complex structure is also observed for Al(Mg) but with a different character to the pattern. This is shown in Fig. 1c.

For the Ag alloy α ≈ 0.07 from 2 to 6K, then rapidly rises to 0.16 at about 15K, dropping off starting a little above 20K to a minimum of 0.12 at 35K followed by a peak of 0.15 at 60K and a further minimum of about 0.06 at 100K and a final slight rise at 180K.

The Al(Zn) data presented in Fig. 1d have the least pronounced structure of all the samples. This may indicate a smaller lattice strain associated with the more readily soluble Zn. The fall off in α at only 4K, compare Al(Mg) Fig. 1c, would indicate a very small binding, possibly with a trap rate comparable to the detrap rate and both sufficiently large to allow motional narrowing from the expected interstitial value for α of 0.44.

A common feature to all our data seems to be a small peak in α of between 0.05 and 0.08 at about 180K.

There is a remarkable insensitivity to heat treatment for all our data. The number and rough position of peaks and valleys remain throughout. At most there may be a narrowing of some of the peaks with annealing. This could indicate that even the rapid quench is too slow to freeze sufficient vacancies to be observed, or that the strain fields induced by the impurities do not allow motion to the vacancies and that the bonding of vacancies and impurities in clusters is sufficiently strong so as to be insensitive to heat treatment.

In the future, several directions could be explored. Very thin samples so as to be able to quench the sample in milliseconds or less would clarify the question of whether or not the cooling rates were fast enough. The use of single crystals and varying the magnetic field would better determine the trapping site. Following an alloy system through known annealing stages including the formation of precipatates would be useful in interpreting the features we are seeing. Certainly the structure is complex and is a challenge to be understood.

IV. Acknowledgements

We would like to thank H. K. Birnbaum, K. G. Petzinger and W. B. Gauster for many helpful discussions. The artistry of S. Hummel with light pipes is gratefully acknowledged. The staff of SREL, even in the cyclotron's last hours, provided truly marvelous support. The work at the College of William and Mary and at George Mason University was supported in part by the NSF and the Commonwealth of Virginia; work at Brookhaven National Laboratory by the Dept. of Energy; work at Virginia State College by NASA.

References

1. W.B. Gauster et al., Solid State Comm. 24, 619 (1977).
2. B.A. Nikol'sky, Meson Chemistry and Mesomolecular Processes in Matter, (Dubna, USSR, 1977).
3. W.J. Kossler et al. Submitted to Phys. Rev. Letters.
4. K. Dorenburg et al. To appear in Zeitschrift für Physik B.
5. W. Schilling and K. Sonnenberg, J. Phys. F: Met. Phys. 3, 322 (1973).
6. C.O. Almbladh et al., Phys. Rev. B14, 2250 (1976); J.K. Norskov, Solid State Comm. 24, 691 (1977).
7. M.S. Shaw, Bull. Am. Phys. Soc. 23, 360 (1978).

Diffusion and Trapping of Positive Muons in Al:Cu Alloys and in Deformed Al

W. J. Kossler, A. T. Fiory, W. F. Lankford, J. Lindemuth, K. G. Lynn, S. Mahajan, R. P. Minnich, K. G. Petzinger, and C. E. Stronach

College of William and Mary, Williamsburg, Virginia 23186, and Bell Laboratories, Murray Hill, New Jersey 07974, and George Mason University, Fairfax, Virginia 22030, and Brookhaven National Laboratory, Upton, New York, 11973, and Virginia State College, Petersburg, Virginia 23803

(Received 8 June 1978)

Depolarization of μ^+ particles implanted into quenched alloys of 0.042, 0.13, and 0.42 at.% Cu in Al shows peaks in the temperature dependence which are attributed to trapping of the muons by various metastable Cu impurity complexes, and provides evidence that positive muons can be used to study impurity correlations in metals.

Previous work has shown complex muon diffusion phenomena in metals.[1-3] This work is a study of one of the simplest systems of dilute impurities in metals which shows interesting muon depolarization dependence on temperature and therefore should be useful in understanding muon trapping and diffusion. For low concentrations of Cu in Al, though precipitation is not observed by transmission electron microscopy (TEM), there is indirect evidence from resistivity[4] and NMR[5] measurements as well as theoretical grounds[6] to suspect that Cu is not uniformly distributed.

To study this low-concentration region, we have measured the depolarization of implanted spin-polarized μ^+ particles (muon spin rotation[7]) in the temperature range 1.7 to 300 K. These experiments with muons provide a unique way of studying the thermal diffusion and transitory trapping processes for implanted particles, as well as the nature of impurities and other defects that act as traps. Over the temperature range studied, the weak depolarization that has been previously reported[8] for high-purity Al is explained by rapid diffusion of the muon.[9] Depolarization has previously been observed in Al:Cu.[10] The present data taken with a finer temperature mesh on quenched Al:Cu alloys reveal previously unobserved peaks in the temperature dependence, which can be explained on the basis of a model involving muon trapping at sites near Cu impurity complexes. So far trapping by impurities has not been treated theoretically. We presume that it arises from the local lattice distortion and electronic perturbation at sites near the impurity.

Alloys containing 0.042, 0.13, and 0.42 at.% Cu were prepared from 99.99%-pure Al and Cu. Eight 0.3-cm×7.5-cm×10-cm plates fabricated from each ingot were combined to make muon-spin-rotation samples. Each plate was given a homogenizing treatment by annealing in air at 820 K followed by a quench (0.1 sec time constant) into agitated brine at 290 K. Prior to measurement, the 0.42% alloy was aged for 1.5 days at 390 K, the 0.13% alloy about 0.5 h at 300 K, and the 0.042% alloy 3 days at 300 K. Stereoscopic TEM measurements find no evidence of precipitation down to 200 nm and find an average dislocation density of 10^9 cm^{-2}.

In order to test the role of point defects and dislocations on muon trapping, we also studied a 99.999%-pure Al sample, deformed 50% in compression at approximately 77 K to a final thickness of 2 cm. Prior to the muon-spin-rotation measurements, the temperature of the sample was kept below 160 K so that vacancies created during deformation would not be lost. Subsequent TEM analysis at room temperature found dislocation cells about 1 μm across, with a dislocation density of 10^9 to 10^{10} cm^{-2}.

The results of the muon-spin-rotation measurements are shown in Fig. 1 and were analyzed in the following manner. The decay of the asymmetry in the muon-spin-rotation signal can be represented as $\exp[-\gamma(t)]$. The muon spin decay rate, which we define as $d\gamma/dt$, has an average value which is statistically weighted according to the radioactive decay law. Thus we can define a dimensionless depolarization parameter:

$$\alpha = \int_0^\infty \exp(-st)(d\gamma/dt)\,dt, \tag{1}$$

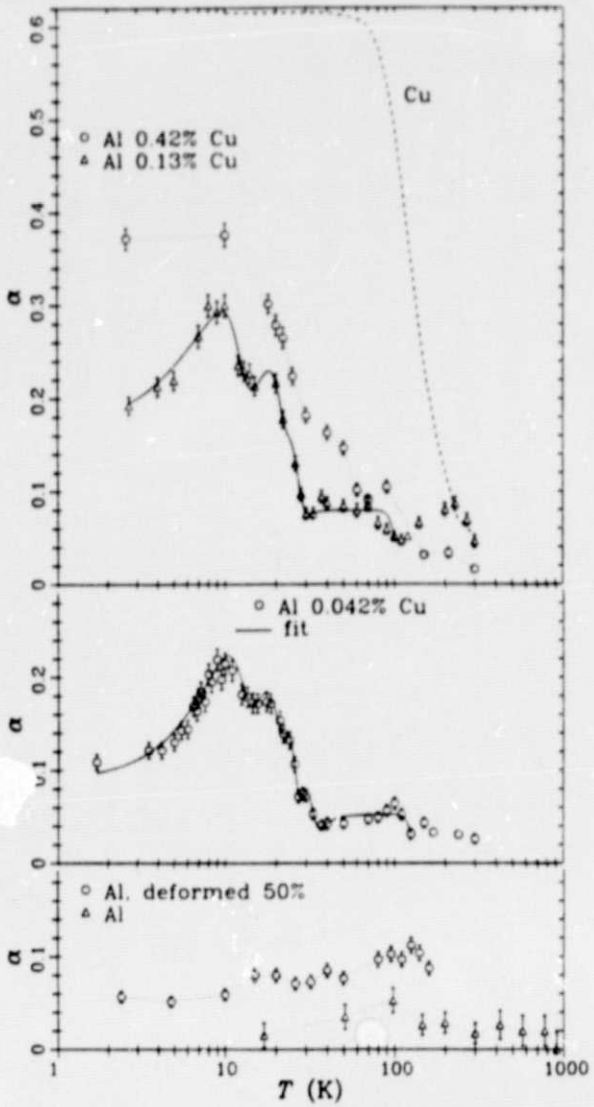

FIG. 1. Temperature dependence of the depolarization parameter α, measured with external fields of 500 Oe for the 0.042% and 0.13% alloys and deformed Al, and 330 Oe for the 0.42% alloy. Data for Cu (Ref. 10, 30 Oe) and Al (Ref. 8, 75 Oe) are uncorrected for weak field perturbations (Ref. 11). The fits are Eq. (5) with the parameters in Table I.

where the muon lifetime $s^{-1} = 2.2\ \mu$sec. We evaluate α by fitting the experimental time histogram with a Gaussian function, $\gamma(t) = \frac{1}{2}\alpha s^2 t^2$, which we find gives a better fit than an exponential. We have chosen to represent the data in terms of the α parameter because α is also conveniently calculated from the theory, discussed below. For comparison, values of α calculated from previous measurements on annealed polycrystalline samples of Al[8] and Cu[12] are also shown in Fig. 1.

The calculated value of α is 0.44 for the muon localized at an octahedral interstitial site and 0.12 for a substitutional site, neglecting lattice relaxation and the finite extent of the muon wave function.[9,11]

Nonlinear screening calculations using the jellium model predict trapping of protons as well as muons at vacancies in Al.[13,14] We had assumed *a priori* that dislocations would also be capable of trapping the muons.

Our results for the deformed Al in the vicinity of 100 K are consistent with the trapping at open volume defects as opposed to trapping at interstitial sites by the strain fields surrounding defects.[15] A smaller fraction of the muons diffuse to traps at lower temperatures, indicating that the diffusion time increases with decreasing temperature.

The depolarization in the alloys at $T \sim 50$ K is sufficiently large to be caused by the trapping of muons at interstitial sites. For the two more dilute alloys α does not reach a constant maximum at low temperatures nor does it drop off smoothly with temperature, as it does for Cu (Fig. 1). In Cu the depolarization at low temperatures is the result of self-trapping at an octahedral interstitial site,[16] and the decrease at high temperatures is attributed to thermal diffusion.[12] The peaks observed in the alloy data at low temperatures increase in magnitude with increasing Cu concentration. This is expected for thermal diffusion of the μ^+ to traps whose population of Cu increases with impurity concentration.[17] What is surprising here is that complex structure is found above 10 K.

A motional-narrowing theory for $\gamma(t)$, related to that used for nuclear magnetic resonance, has been proposed[17,18] to explain muon diffusion and trapping in terms of correlation functions:

$$\gamma(t) = \sum_i \sigma_i^2 \int_0^t dt' \int_0^{t'} dt'' F_i(t'') G_i(t' - t''). \qquad (2)$$

The sum extends over all interstitial sites in the sample, each having a local frequency distribution of second moment σ_i^2 from nuclear dipolar fields. $F_i(t)$ is the probability that the muon occupies site i at time t and $G_i(t)$ is the site autocorrelation function. Equation (2) can be rewritten to represent equivalent unperturbed sites in the host and n types of trapping sites. The result is similar to Eq. (2), where we now define f_0 as the probability that *any* host site is occupied, and f_m for $m = 1, \ldots, n$ as the probability that a trap of type m of concentration c_m is occupied. A

good approximation[18] to the autocorrelation function for any site of type m is $g_m = \exp(-p_m t)$. When the traps are assumed to be dilute, the f_m are then solutions to the following rate equations:

$$\frac{df_0}{dt} = -p_0 f_0 + \sum_{m=1}^{n} p_m f_m \quad [f_0(0) = 1 - c], \tag{3}$$

$$\frac{df_m}{dt} = p_0 c_m f_0 - p_m f_m \quad [f_m(0) = c_m;\ m \neq 0], \tag{4}$$

where $c = \sum_m c_m$. The renormalized jump rate between host sites is p_0. The p_m for $m > 0$ are detrapping rates given as $p_m = p_0 \exp(-H_m/kT)$, with H_m the binding enthalpy to the trapping site. Actual lattice structure is not taken into account explicitly in this model.

Since our definition of α is identical to the Laplace transform, the solution for α can be expressed as

$$\alpha = \sum_{m=0}^{n} \sigma_m^2 \tilde{f}_m(s)/(s + p_m), \tag{5}$$

where $\tilde{f}_m(s)$ is the transform of $f_m(t)$. Thus one can solve the theoretical Eq. (2) quite easily as one does not need to solve the integral convolution of this equation in the time domain. Since the depolarization in pure Al is small, $p \gg s$ and the $m = 0$ term is negligible. The model predicts a peak in the temperature dependence of α when p_0 increases monotonically with temperature and the trapping times and detrapping lifetimes are comparable to the muon lifetime, i.e., when the conditions $p_0 c_m \approx s$ are satisfied. Thus, the peak appearing at the lowest temperature is associated with traps present in the highest concentration, assumed to be a single Cu impurity. The additional peak structure observed at higher temperatures is due to a lower concentration of traps with higher binding enthalpies, assumed to be di- and tri-Cu clusters.

Equation (5) was used to fit the data on the alloys for $T \leq 100$ K using a nonlinear least-squares procedure with $n = 5$. Because of a lack of a quantitative theoretical treatment, we have used an empirical formula for the temperature dependence of p_0:

$$p_0 = a \exp(-H_0/kT) + b + dT^2, \tag{6}$$

where the three terms are to represent the following. At high temperatures the Flynn-Stoneham model[19] predicts an Arrhenius dependence and at low temperatures a constant that is proportional to the coherent tunneling rate plus a one-phonon-assisted tunneling term that is linear in temperature and dependent upon strain broadening. We find that the dT^2 term fits the data better than a linear term. The fitted parameters are given in Table I. For the highest-concentration alloy (0.42%) the total number of traps is sufficiently high that the contribution of the individual traps is more difficult to observe and the data therefore were not fitted.

The significance of these results is that qualitatively our model describes the data at low temperatures. Quantitatively, the binding enthalpies giving rise to the trapping at low temperatures are quite small. The concentration of traps producing the peak at 10 K is consistent with individual Cu impurity traps. The structure seen at $T > 10$ K is attributed to appreciable concentrations of microclusters of two or more Cu. We note that if the distribution of impurities were random, the fraction of interstitial sites with more than one Cu nearest neighbor would be about two to three orders of magnitude smaller than the fraction with one neighbor. Our larger fractions indicate that clustering is energetically more favorable even at these low Cu concentrations.

The depth of the $m = 5$ trap requires a different interpretation. On the basis of our findings for the deformed Al and our TEM results, we suspect that dislocations are responsible for the structure observed at temperatures near 100 K. This is also consistent with our small σ_m parameter. Diffusion along these dislocations explains the smaller depolarization at 300 K.

The results of this Letter are the first evidence demonstrating that positive muons provide a unique way of studying impurity correlations in

TABLE I. Results of fitting α, given by Eq. (5), to the data. Because of correlations between parameters, values are determined to order-of-magnitude accuracy, except for the binding enthalpies where shown. The parameters in Eq. (6) are $a = 2.6 \times 10^{14}$ sec^{-1}, $b = 2.1 \times 10^{8}$ sec^{-1}, $d = 7.8 \times 10^{6}$ sec^{-1} K^{-2}, and $H_0 = 22$ meV.

Alloy (%)	m	σ_m (10^5 sec^{-1})	c_m (ppm)	H_m (meV)
0.042	1	3	410	9(5)
	2	3	180	16(7)
	3	3	48	22(15)
	4	3	4	36(20)
	5	1	4	200(60)
0.13	1	3	910	9
	2	3	510	18
	3	3	110	25
	4	3	40	28
	5	1.3	180	160

metals. Extension of this work to other impurities in Al is currently in progress.

The authors acknowledge beneficial conversations with W. B. Gauster, R. L. Munjal, T. McMullen, E. Zaremba, and B. Lengeler, and the technical assistance of R. Manners. The experiments were carried out at the Space Radiation Effects Laboratory's synchrocyclotron. This work was supported in part by Bell Laboratories, the Commonwealth of Virginia, the U. S. Department of Energy, the National Aeronautics and Space Administration, and the National Science Foundation.

---

[1]V. G. Grebinnik *et al.*, Pis'ma Zh. Eksp. Teor. Fiz. 25, 322 (1977) [JETP Lett. 25, 298 (1977)].

[2]H. K. Birnbaum *et al.*, Phys. Rev. B 17, 4143 (1978).

[3]M. Borghini *et al.*, Phys. Rev. Lett. 40, 1723 (1978).

[4]T. Federighi, in *Lattice Defects in Quenched Metals*, edited by F. M. J. Cotterill *et al.* (Academic, New York, 1965), p. 217; B. Lengeler, private communication.

[5]L. E. Drain, Phys. Rev. B 8, 3628 (1973).

[6]G. K. Straub, A. R. DuCharme, and J. R. Holland, Solid State Commun. 15, 1901 (1974).

[7]A. Schenck, in *Nuclear and Particle Physics at Intermediate Energies*, edited by J. B. Warren (Plenum, New York, 1975), p. 178.

[8]W. B. Gauster *et al.*, Solid State Commun. 24, 619 (1978), and references therein.

[9]M. S. Shaw, Bull. Am. Phys. Soc. 23, 360 (1978).

[10]B. A. Nikol'sky, Meson Chemistry and Mesomolecular Processes in Matter, Dubna, U. S. S. R., 1977 (to be published); V. G. Grebinnik *et al.*, Pis'ma Zh. Eksp. Teor. Fiz. 27, 33 (1978) [JETP Lett. 27, 30 (1978)].

[11]The Zeeman energy is expected to exceed electric quadrupole splittings for ^{27}Al near the μ^+ and Cu (Ref. 5) impurities. Electric field gradients and the location of the muon can be determined from the magnetic field dependence for single crystals. [See P. Jena *et al.*, Phys. Rev. Lett. 40, 264 (1978); and O. Hartmann, Phys. Rev. Lett. 38, 832 (1977).] In weak fields α may be a factor 5/3 larger.

[12]V. G. Grebinnik *et al.*, Zh. Eksp. Teor. Fiz. 68, 1548 (1976) [Sov. Phys. JETP 41, 777 (1978)].

[13]P. Jena, private communication.

[14]Z. D. Popović *et al.*, Phys. Rev. B 13, 590 (1976).

[15]J. P. Bugeat *et al.* [Phys. Lett. 58A, 127 (1976)] have proposed that implanted protons are trapped at tetrahedral sites near vacancies.

[16]M. Camani *et al.*, Phys. Rev. Lett. 38, 836 (1977).

[17]K. G. Petzinger, R. L. Munjal, and E. Zaremba, to be published.

[18]T. McMullen and E. Zaremba, Phys. Rev. B 18, 3026 (1978).

[19]C. P. Flynn and A. M. Stoneham, Phys. Rev. B 1, 3966 (1970).

PHYSICAL REVIEW B VOLUME 18, NUMBER 7 1 OCTOBER 1978

Dynamic field on 40-MeV μ^+ traversing magnetized iron

J. M. Brennan, N. Benczer-Koller, and M. Hass*
Rutgers University, New Brunswick, New Jersey 08903

W. J. Kossler and J. Lindemuth
The College of William and Mary, Williamsburg, Virginia 23186

A. T. Fiory, D. E. Murnick, and R. P. Minnich
Bell Laboratories, Murray Hill, New Jersey 07974

W. F. Lankford
George Mason University, Fairfax, Virginia 22030

C. E. Stronach
Virginia State College, Petersburg, Virginia 23803
(Received 1 February 1978)

Previous experiments have demonstrated the existence of large dynamic magnetic fields that act on positive heavy ions traversing magnetized iron. These studies have been extended to the limit of ionization and to $v/c = 0.68$ by using spin-polarized muons. The angular precession of the spin of μ^+ particles which traversed magnetized-iron plates and stopped in aluminum was measured. Decay positrons were detected at 0°, 90°, and 270°. Relative phases of the corresponding muon-spin-rotation spectra were obtained as a function of the magnetization direction in the iron. After subtracting the phase shift resulting from the saturation magnetization in the iron and the fringing fields, the experimental result for the dynamic field $\Delta B = -0.5 \pm 2.6$ kG is obtained, in agreement with theoretical expectations for very fast totally stripped ions.

INTRODUCTION

The existence of an intense transient magnetic field acting on fast ions slowing down in magnetic media was discovered in 1968 by Borchers *et al.*[1] The transient field was theoretically described by Lindhard and Winther[2] in 1971 in terms of scattering of polarized electrons in the ferromagnetic medium by the moving ions. Hubler *et al.*[3] in 1974 parametrized the Lindhard and Winther model using existing data for medium-weight ions of low initial velocity, $v/c \lesssim 0.01$. In this model, the field varies inversely with the ion's velocity for $v/c \gtrsim 0.004$, is constant at lower velocity ($0.0005 \lesssim v/c \lesssim 0.004$) and vanishes at low velocity.

In recent measurements[4-10] on faster ions, a dynamic field much larger than that predicted by the adjusted Lindhard-Winther theory[3] was observed and, within the velocity range studied, the field increases with the ion's velocity through the medium. This field was qualitatively described in terms of polarized-electron capture into electron vacancies produced in the moving ion.[8] A recent review of the subject has been given by van Middelkoop.[11]

Experiments have been carried out at the Rutgers-Bell tandem accelerator on ^{56}Fe, ^{82}Se, ^{106}Pd, and ^{112}Cd ions in iron and on ^{82}Se ions in gadolinium in the velocity range $0.01 \lesssim v/c \lesssim 0.05$. In these experiments, the ions were excited to their 2^+ state by a beam of 72-MeV $^{32}S^{8+}$ ions, recoiled through the ferromagnetic foil and stopped in a copper backing where they decayed in an environment free of perturbations. The precession of the angular correlation of the deexcitation γ rays was measured as a function of the direction of polarization of the ferromagnetic material. As the g factor of these states was known, the velocity and Z dependence of the magnetic field was determined. The results obtained with the heavier ions show unambiguously that the dynamic field which acts on the ions studied *increases* with the velocity of the ion. The observed dynamic field has been phenomenologically described by a function of the velocity and atomic number of the ion[5,8]:

$$B(Z, v) = aZ^{3/2}(v/v_0)\mu_B N_p , \tag{1}$$

where $v_0 = e^2/\hbar$, N_p is the polarized-electron density and μ_B is the Bohr magneton. For iron $\mu_B N_p = 1752$ Oe and $a = 12 \pm 0.5$.

An alternate parametrization in terms of the effective charge of the ion passing through the magnetic material fits the data equally well:

$$B(z, v) = a' Z_{\text{eff}}^{3/2} \mu_B N_p , \tag{2}$$

where

$$Z_{\text{eff}} = Z[1 - \exp(-v/v_0 Z^{0.54})] \tag{3}$$

is the best fit to the observed effective charge of ions leaving a solid foil,[12] and $a' = 140 \pm 8$.

In both parameterizations, the field depends on the type of ferromagnet only through the number of polarized electrons per unit volume, suggesting that atomic shell or band-structure effects may not play a significant role for heavier ions.

As the nature of the dynamic field—a hyperfine interaction between the partially stripped ion and the magnetized medium—is not yet fully understood, it is not at all evident that the parametrization of the field which seems to fit the data in the velocity range $0.01 \lesssim v/c \lesssim 0.05$, should extend to higher velocity. At velocities greater than Zv_0, where the ions are completely stripped, the solid can probably be treated as a gas of polarized electrons and a dynamic magnetic field inversely proportional to the ion velocity should result.[2,13]

In order to test the validity of the charge and velocity dependence of the alternate parametrizations, high velocity, totally stripped ions should be used. For this purpose, the effect of the dynamic field on polarized positive muons traversing a thin magnetized iron plate was investigated.

Previous studies using the spin precession of muons stopped in unmagnetized iron have found that the field is 3.6 kG at room temperature, for a sample in zero external field.[14,15] This field is explained in terms of a dipolar contribution from the iron ions and a contact interaction with the polarized screening electrons.[16] These results imply that the dynamic field on the muon is not very large. Otherwise the residual polarization of the muon's spin would have been lost on traversing the unmagnetized iron, washing out the spin precession signal of the stopped muon.[15]

In the present experiment, the effects on muons which traverse a magnetized iron plate and subsequently stop in an aluminum target located in a fixed externally applied magnetic field were observed. The angle through which the spin has precessed in the iron is detected as a phase shift in the oscillatory μSR (muon spin rotation) spectra of the stopped μ^+.[17]

EXPERIMENTAL PROCEDURE

The experiment was carried out with the apparatus shown schematically in Fig. 1. Positive pions are produced at an internal target in the SREL (Space Radiation Effects Laboratory) synchrocyclotron[18] and focused into an external meson channel. The momentum analyzing magnet M is adjusted to select μ^+ particles which originate from π^+ decays in the backwards direction in the π^+ frame of reference. The π^+ decays produce a beam of spin polarized muons, a well-known consequence of parity nonconservation in weak interactions. The arrangement of charged particle scintillation detectors is also shown in Fig. 1. Figure 2 shows the measured particle flux at detector A as a function of momentum, as determined by varying the current through the deflecting magnet M. The μ^+ beam passes through a magnetized Fe plate in the reversible magnet $C1$, and stops in an Al target located in a constant magnetic field produced by magnet $C2$.

The logic coincidence $AB\bar{F}$ establishes that a μ^+ stopped in the target. The mean momentum of the incident μ^+ beam, 103 MeV/c, was deduced from the range measurements shown in Fig. 3, using the known momentum dependence of the muon's range in various materials.[19] The mean kinetic energy of the incident beam is 42 MeV and the

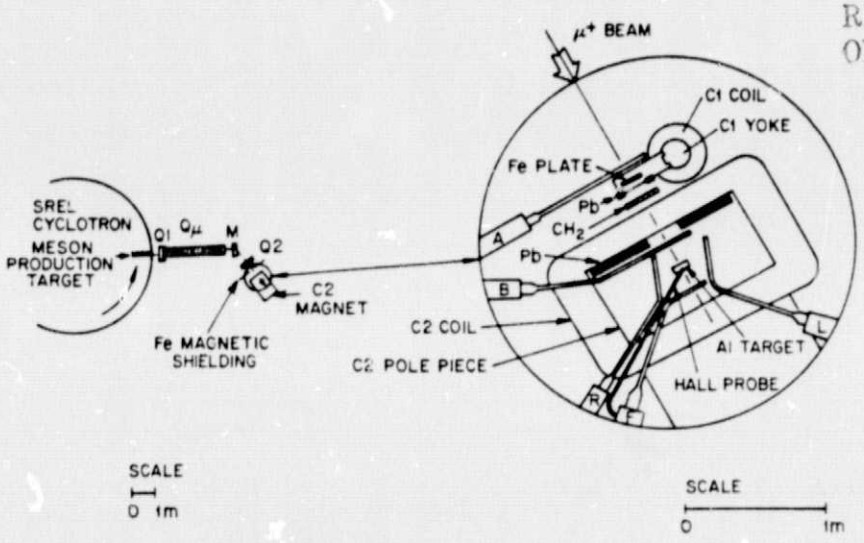

FIG. 1. Layout of the meson channel at SREL and the μSR apparatus in the target area. $Q1$ and $Q2$ are input and output quadrupole magnets, $Q\mu$ the "drift tube" where the pions decay into muons, and M the momentum selection magnet. The gap of magnet $C2$ is 30 cm. The Al stopping target is located 55 cm downstream from the Fe plate.

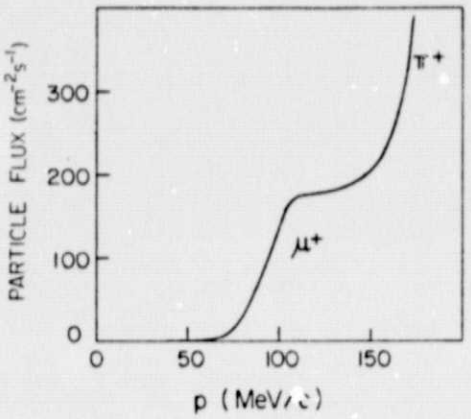

FIG. 2. Total particle flux at the output of the meson channel. The *M* magnet current settings have been converted to an approximate momentum scale. The shoulder at 100 MeV/*c* results from the backwards decay muons. The pion peak occurs at about 230 MeV/*c*.

mean velocity is 0.68*c*. Two range curves are shown, for the aluminum stopping target used for the phase-shift measurement, and the other for a thinner Cu target. The width of the momentum distribution is determined more accurately with the Cu target. The momentum spread is about ±8 MeV/*c*, corresponding to a velocity spread of ±0.03*c*. The experiment was carried out separately for different Fe plates of thicknesses varying from 0.1 to 0.8 cm inserted in the *C*1 magnet. The mean velocity of the muons in the Fe was decreased by up to 6%. The energy of the muon beam hitting the target was kept approximately constant by adding appropriate amounts of CH_2 degrader to compensate for the thinner Fe plates.

The iron plates were fabricated from 99.99% Fe, machined into sheets 12.7-cm square and 0.05- to

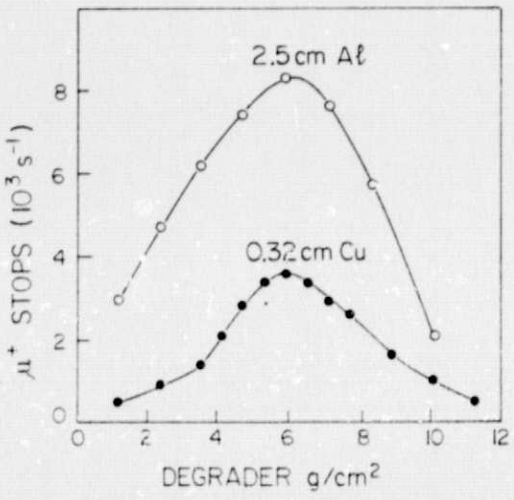

FIG. 3. Muon stopping rate in Al and Cu targets vs thickness of CH_2 degrader placed in front of the target.

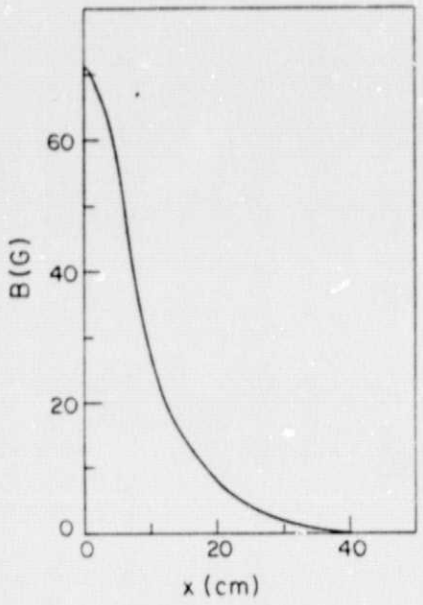

FIG. 4. Axial variation of the vertical component of the field produced by the *C*1 magnet along the beam direction.

0.04-cm thick and subsequently annealed. The electromagnet *C*1 has a movable iron yoke that mates evenly against the edges of the plates. The direction of the magnetization of the Fe plate is vertical. The magnetic induction in the plate was measured by integrating the voltage produced in a sense coil wound around the plate as the *C*1 magnet is energized. For 1600 ampere-turns a magnetic induction of 16 kG is produced in the plate. The profile of the fringing field outside the plate was mapped along the beam axis, and is shown in Fig. 4. The fringing field was insensitive to the Fe plate thickness in the range 0.1–0.8 cm.

The muon beam was collimated to an approximately 12-cm square aperture by the *C*1 magnet yoke and additional 5-cm thick Pb shields placed at each side of the Fe plate. The profile of the μ^+ beam at the Al target position (Fig. 5) was scanned horizontally in the direction transverse to the beam, for the two directions of magnetization of the Fe plate with a 2.5-cm square scintillation detector. These measurements show a bending of the beam, due mainly to the deflection in the magnetization field in the Fe plates and to a lesser extent to the fringing field. For an Fe plate of thickness d_{Fe} a bending angle φ_B may be calculated from the measured magnetization and fringing fields:

$$\varphi_B = (0.067\ \text{cm}^{-1}) d_{Fe} + 0.006 . \quad (4)$$

The aluminum target was 5-cm wide by 10-cm high and 2.5-cm thick. The local field at the tar-

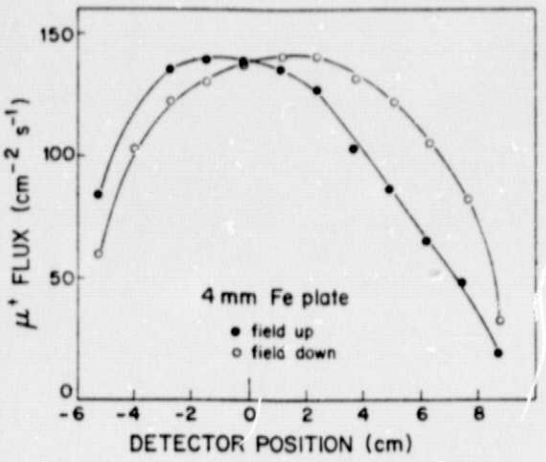

FIG. 5. Scans of the muon beam intensity, taken with a 2.5-cm square detector located at the Al target position and moved along the horizontal transverse direction. "up" and "down" refer to the direction of the magnetization of the Fe plate.

get was 105 Oe. Magnetic shims were positioned near the pole tips of $C2$ in order to produce a homogeneous field at the target. The root-mean-square variation in the field was 0.1 G over the target volume, with the $C1$ magnet off. Maps of the local-field distribution were also made when $C1$ was turned on, for both polarities of the $C1$ current. A small nonlinear variation in the field was found in the horizontal plane, which resulted in a 0.03-G shift of the average field with respect to the field at the center of the target. This field was held constant by adding an extra coil on the $C2$ magnet which was energized by a feedback signal from a Hall-effect probe inserted into a 0.6-cm hole drilled to the center of the target. The field at the center of the target varied by less than 0.01 G as the $C1$ current was reversed.

Positron decays in the 0°, 90°, and 270° directions with respect to the beam direction were detected by the scintillators F, L, and R shown in Fig. 1. At a time t after the μ^+ stops in the target, a positron decay event in one of the three directions is indicated by the logic coincidence $F\bar{A}\bar{B}$, $L\bar{A}\bar{B}$, or $R\bar{A}\bar{B}$, respectively. Six spectra of events versus time were recorded in a multichannel analyzer corresponding to the three positron detectors and the two directions of the Fe magnetization. The total event rate after μ^+ and e^+ pile-up rejection was about 10^3 $\sec^{-1}$. The direction of $C1$ was reversed, and the data acquisition was momentarily disabled, after each increment of 2×10^5 events. The data acquisition system included a magnet controller, actuated by a presettable scaler, and a PDP 11/10 computer. The muon stop and event rates were continuously monitored. The true zero of time was periodically recorded by detecting prompt signals associated with scattered muons. The timing calibration of the analyzer was also checked before and after each run. A low magnetic field in $C2$ is desirable since spurious phase shifts originating from electronic timing drifts increase in proportion to the spin precession frequency.

Several runs were carried out on each of a variety of Fe plates 0.1-, 0.4-, 0.6-, and 0.8-cm thick, respectively. The spectra corresponding to either of the three detectors at 0°, 90°, or 270° were fitted using a nonlinear least-squares method[20] with the following model μSR function.

$$N(t)=A_+e^{-t/\tau}\{1+a_+e^{-\lambda t}\cos[(\omega\pm\Delta\omega)t + \varphi\pm\Delta\varphi]\}+B_+ , \qquad (5)$$

where (+) or (−) applies to the spectra for the two directions of Fe plate magnetization. The fitting procedure treats A_+, A_-, a_+, a_-, λ, ω, $\Delta\omega$, φ, $\Delta\varphi$, B_+, and B_- as 11 adjustable parameters. The muon lifetime $\tau=2.1994$ μsec is used.

The parameters $a_\pm$ give the magnitude of the asymmetry, which depends upon geometrical details such as the polarization of the muon beam and the selectivity in the e^+ detection. These effects are illustrated in Fig. 6, where the asymmetry measured for a thin Cu target is shown as a function of the incident μ^+ momentum as determined by the thickness of the degrader interposed in the beam. The results display the dependence of the asymmetry upon the average momentum of the stopped μ^+ and the target thickness, which affect the energy of the emitted e^+. The angle φ is an average geometric angle determined by the average initial spin orientation of the μ^+ beam and the location of the positron detector. The angular precession frequency of the stopped muons is $\omega=\gamma_\mu\times105$ G $=9.0\times10^6$ $\sec^{-1}$. The factor $\exp(-\lambda t)$ takes into account the inhomogeneity in the local field in the target.

The phase-shift parameter $\Delta\varphi$ gives the change

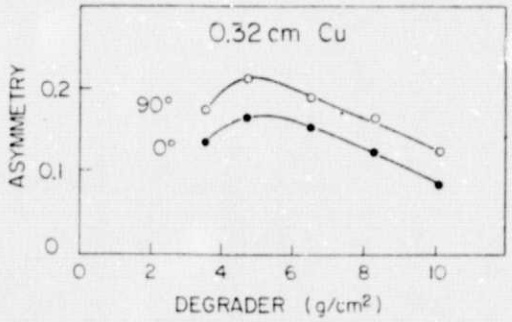

FIG. 6. Positron decay asymmetry measured as a function of the CH_2 degrader thickness.

TABLE I. Fitted parameters for the 0.4-cm thick Fe plate, according to Eq. (5). Statistical errors in the least significant figures are given in parentheses.

	0°	90°	270°
Events	1.1×10^7	1.7×10^7	1.5×10^7
a_+	0.140(1)	0.169(1)	0.157(1)
a_-	0.140(1)	0.173(1)	0.154(1)
$\lambda(10^4\ \mathrm{sec}^{-1})$	4.0(3)	4.6(3)	3.9(3)
$\omega(10^6\ \mathrm{sec}^{-1})$	8.979(4)	8.957(3)	8.958(3)
$\Delta\omega(10^6\ \mathrm{sec}^{-1})$	0.002(4)	−0.001(3)	−0.008(3)
φ	−0.316(8)	−1.801(8)	1.145(8)
$\Delta\varphi$	0.021(9)	0.021(7)	0.034(8)

in the spin orientation of the muon beam produced by the magnetization and dynamic fields in the Fe plate and the fringing field. Both the magnitude and the statistical uncertainty in $\Delta\varphi$ are insensitive to the sampling time interval of the multichannel analyzer and to the magnitude of the field on the Al target. This result was deduced from the analysis of model simulations of the experiment. The parameter $\Delta\omega$ was included in the model function in order to account for a possible small change in local field when C1 is reversed. The parameter $\Delta\varphi$ is strongly correlated with $\Delta\omega$, the correlation coefficient being 0.8. The correlation coefficients between $\Delta\varphi$ and the other parameters have magnitudes less than 0.1. Typical values obtained for the 0.4-cm Fe plate are given in Table I, while the phase shifts obtained for the other thicknesses of Fe are displayed in Table II.

An alternate procedure was also tested, whereby $\Delta\omega$ was set to 0 and 10 adjustable parameters were varied. This analysis did not produce statistically significant changes in $\Delta\varphi$, although the statistical errors in $\Delta\varphi$ were reduced by 40%. In the 11-parameter fits, the $\Delta\omega$ values were smaller than the statistical errors in $\Delta\omega$.

DISCUSSION OF THE RESULTS

As the muon velocity in the iron is approximately constant, the phase shift is proportional to the time spent in the iron plate and hence varies linearly with the thickness of the plate:

$$\Delta\varphi = r d_{Fe} + \Delta\varphi_0 . \tag{6}$$

The slope r and the intercept $\Delta\varphi_0$ were obtained from a linear least-squares fit and are given in Table III. The results for the 11-parameter fitting procedure appear to be more consistent, and were adopted as the better representation of the results. There does not appear to be a systematic influence of the beam bending, since the three detectors give the same precession angle within the statistical error. The geometric effect caused by the lateral deflection of the beam was expected to be maximum for the 0° detector, where it would tend to increase $\Delta\varphi$. The width of the Al target was chosen to be narrow compared to the width of the muon beam, in order to minimize this effect. The magnitude of the beam bending influence was estimated in a model calculation where beam profiles such as the typical one shown in Fig. 5 were assumed to represent the spatial distribution of stopped muons in the target. The calculation neglected positron scattering and attenuation in the target and a small inhomogeneity known to exist in the efficiency of the scintillator. The calculation gives a geometric contribution to the phase-shift parameter r of 0.001 cm^{-1}, which is near the limit of detection.

The net precession angle averaged over the three detectors is plotted against the Fe plate thickness in Fig. 7. The solid line represents the linear least-squares fit. From the slope $r = 0.065 \pm 0.011$ cm^{-1} of the fitted line and the average muon velocity of $v = 0.68c$, the net field on the muon is ob-

TABLE II. Experimental phase shifts $\Delta\varphi$ obtained for the various thicknesses of Fe plate.

d_{Fe} (cm)	$\Delta\varphi$(mrad) 0°	90°	270°
0.1	8(11)	−1(9)	9(10)
0.4	21(9)	23(7)	34(8)
0.6	41(12)	23(10)	32(12)
0.8	49(11)	49(10)	59(11)

TABLE III. Results of fitting the μSP phase-shift measurement of $\Delta\varphi$ to the linear relation given in Eq. (6). The slope r is given in milliradians/cm and the intercept $\Delta\varphi_0$ in milliradians.

Method	Parameters	0°	90°	270°	Average
$\Delta\omega$ variable	r	64(20)	65(18)	65(20)	65(11)
$\Delta\omega$ variable	$\Delta\varphi_0$	−2(11)	−7(9)	4(10)	−1(6)
$\Delta\omega = 0$	r	51(13)	63(12)	55(12)	56(7)
$\Delta\omega = 0$	$\Delta\varphi_0$	5(7)	−5(6)	1(6)	0(4)

REPRODUCIBILITY OF THE ORIGINAL PAGE IS POOR

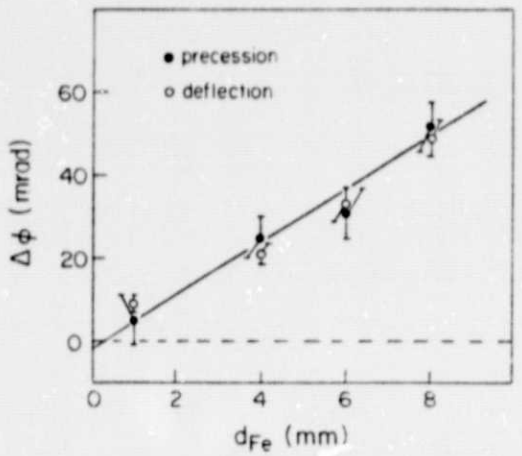

FIG. 7. Muon spin precession angle (phase shift in the μSR fits, open circles) averaged over the three spectra as a function of the thickness of the Fe plate. The least-squares fit (solid line) and the measurements of the beam deflection angles (filled circles) are also shown.

tained:

$$B = rv/\gamma_\mu = 15.5 \pm 2.6 \text{ kG}.$$

Since the stauration field in the Fe plates used was 16.0 kG, the dynamic field enhancement is

$$\Delta B = -0.5 \pm 2.6 \text{ kG}.$$

Thus the observed precession can be explained entirely in terms of the magnetization field. If this result were precisely true, and since $g \approx 2$ for the muon, the beam deflection and spin precession angles must be equal. For comparison, the beam deflection angles calculated from plots such as the one shown for the 0.4-cm plate in Fig. 5 have also been plotted in Fig. 7. These results are consistent with $\Delta B \approx 0$.

In Table IV the values for ΔB resulting from the parametrizations of the dynamic field obtained from heavy-ion reactions, and from the theoretical calculations of Sak and Bruno are listed. If the extrapolation based upon Eq. (1) were applicable here, the field would be proportional to the velocity of the muon, and the resulting phase shift would in turn be proportional to the Fe plate thickness d_{Fe}:

$$\Delta\varphi = \int \gamma_\mu B\, dt = \gamma_\mu a Z^{3/2} \mu_B N_e \int \frac{v}{v_0}\frac{dx}{v}$$

$$= \gamma_\mu a Z^{3/2} \mu_B N_e d_{Fe}/v_0 .$$

This phase shift turns out to be $(8.2 \text{ cm}^{-1}) d_{Fe}$ radians—a rather dramatic prediction. The data easily rule out such an extrapolation of the field to high velocity.

Although we do not have a precise measure of the dynamic field, our result is in agreement with the Sak and Bruno prediction[13] for $v \gg v_0 Z$:

$$\Delta B = 4\pi Z \mu_B N_e v_0/v . \tag{7}$$

Lindhard and Winther did not acutally evaluate the enhancement of the magnetic field at high velocity. Their theory was designed to explain the large magnetic fields acting on relatively slow ($v \ll Z v_0$) ions. For this reason, they assume the field is approximately spherically symmetric and neglect the asymmetric corrections represented in their notation by the parameter ξ. These corrections are, however, important at high velocity. Hence the Lindhard-Winther theory is not directly applicable to fast ions or muons. Furthermore, even though in principle their theory could apply to slow ions, they also neglect atomic shell effects and assume that the ions are essentially stripped. Shell effects can be neglected only for swift ions with $v \gg v_0 Z$, hence in just the region where the asymmetry corrections are important.

It would be very interesting to fill in the large gap in velocity between the present muon experiment and the heavy-ion experiments. The two experiments taken together indicate that there is a maximum in the velocity dependence of the dynamic field. However, the possibility exists that the large dynamic field observed with heavy ions may partly be due to atomic effects such as equilibrium between hole production and capture of polarized electrons from the medium. Experiments on very slow muons ($v \lesssim v_0$) and on very fast totally stripped heavy ions ($v \gtrsim Z v_0$) may be necessary for a better understanding of the dynamic field.

In conclusion we mention two examples of related work with positive muons. It is known that the μ^+ picks up a bound electron in semiconductors and insulators, forming a muonium atom. Recently, a muonium stage for μ^+ stopping in a Ge

TABLE IV. Calculation of the dynamic field and ensuing total phase shifts $\Delta\varphi$ for muons at $v/c = 0.68$, or $v/v_0 Z = 93$, based on three proposed parametrizations of the dynamic field. The saturation field of the iron was taken as 16 kG, the measured value for the iron plates used in the experiment.

	ΔB (kG)	$\Delta\varphi/d_{Fe}$ (cm^{-1})
Dynamic field Eq. (1)	1530	5.96
Dynamic field Eq. (2)	178	0.73
Sak and Bruno Eq. (7)	0.17	0.0063
Experiment	< 2.6	

crystal has been observed through a measurement of the phase shift in the μSR signal associated with muonium precession in a transverse external field.[21] Also, our results show that magnetized solid Fe deflectors and lenses may indeed be used for the transport and focussing of high-energy muon beams without significant loss of polarization.[22]

ACKNOWLEDGMENTS

This work was supported in part by the NSF, the Commonwealth of Virginia, and NASA.

---

*Present address: Weizmann Institute, Rehovot, Israel.

[1]R. R. Borchers, B. Herskind, J. D. Bronson, L. Grodzins, R. Kalish, and D. E. Murnick, Phys. Rev. Lett. 20, 424 (1968).

[2]J. Lindhard and A. Winther, Nucl. Phys. A 166, 413 (1971).

[3]G. K. Hubler, H. W. Kugel, and D. E. Murnick, Phys. Rev. C 9, 1954 (1974).

[4]M. Hass, J. M. Brennan, H. T. King, T. K. Saylor, and R. Kalish, Phys. Rev. C 14, 2119 (1976).

[5]J. M. Brennan, N. Benczer-Koller, M. Hass, and H. T. King, Hyperfine Interactions 4, 268 (1978).

[6]N. Benczer-Koller, M. Hass, J. M. Brennan, and H. T. King, J. Phys. Soc. Jpn. 44, 341 (1978).

[7]J. L. Eberhardt, G. Van Middelkoop, R. E. Horstman, and H. A. Doubt, Phys. Lett. B 56, 329 (1975).

[8]J. L. Eberhardt, R. E. Horstman, P.C. Zalm, H. A. Doubt, and G. Van Middelkoop, Hyperfine Interactions 3, 195 (1977).

[9]M. Forterre, J. Gerber, J. P. Vivien, M. B. Goldberg, K.-H. Speidel, and P. N. Tandon, Phys. Lett. B 55, 56 (1975).

[10]C. Fahlander, K. Johansson, E. Karlsson, and G. Possnert, Hyperfine Interactions 4, 278 (1978).

[11]G. van Middelkoop, Hyperfine Interactions 4, 238 (1978).

[12]H. D. Betz, Rev. Mod. Phys. 44, 465 (1972).

[13]J. Sak and J. Bruno (private communication).

[14]M. L. G. Foy, N. Heiman, W. J. Kossler, and C. E. Stronach, Phys. Rev. Lett. 30, 1064 (1973).

[15]I. I. Gurevich, A. I. Klimov, V. N. Maiorov, E. A. Meleshko, B. A. Nikol'skii, V. I. Selivanov, and V. A. Suetin, Zh. Eksp. Teor. Fiz. 69, 439 (1975). [Sov. Phys. -JETP 42, 222 (1976)].

[16]P. F. Meier, Solid State Commun. 17, 987 (1975).

[17]For a review of the μ SR technique, see A. Schenck, *Nuclear and Particle Physics at Intermediate Energies*, edited by J. B. Warren (Plenum, New York, 1975). p. 176.

[18]The Space Radiation Effects Laboratory, Newport News, Virginia 23606. A description of an earlier version of the SREL meson channel has been given by H. O. Funsten, Nucl. Instrum. Methods 94, 443 (1971).

[19]Lawrence Berkeley Laboratory Report No. UCRL-2426, 1966, revised (unpublished).

[20]D. W. Marquardt, J. Soc. Indust. Appl. Math. 11, 431 (1963).

[21]V. I. Kudinov, E. V. Minaichev, G. G. Myasischeva, Yu. V. Obukhov, V. S. Roganov, G. I. Savel'ev, V. M. Samoilov, and V. G. Firsov, Pis'ma Zh. Eksp. Teor. Fiz. 21, 49 (1975) [JETP Lett. 21, 22 (1975)].

[22]J. Lebritton, F. Lobkowicz, S. C. Melissinos, and W. Metcalf, Nucl. Instrum. Methods 141, 81 (1977).